STRUCTURAL CHEMISTRY

ISSN 2053-2296

A three-step pathway from (2-aminophenyl)-chalcones to novel styrylquinoline–chalcone hybrids: synthesis and spectroscopic and structural characterization of three examples

Diana R. Vera,[a] Juan P. Mantilla,[a] Alirio Palma,[a] Iván Díaz Costa,[b] Justo Cobo[b] and Christopher Glidewell[c]*

[a]Laboratorio de Síntesis Orgánica, Escuela de Química, Universidad Industrial de Santander, AA 678, Bucaramanga, Colombia, [b]Departamento de Química Inorgánica y Orgánica, Universidad de Jaén, 23071 Jaén, Spain, and [c]School of Chemistry, University of St Andrews, Fife KY16 9ST, United Kingdom. *Correspondence e-mail: cg@st-andrews.ac.uk

Received 31 October 2022
Accepted 22 November 2022

Edited by A. G. Oliver, University of Notre Dame, USA

Keywords: synthesis; quinoline; styrylquinoline; chalcone; NMR spectroscopy; crystal structure; molecular structure; molecular conformation; hydrogen bonding; π–π stacking interactions; supramolecular assembly.

CCDC references: 2221749; 2221750; 2221751

Supporting information: this article has supporting information at journals.iucr.org/c

Three new styrylquinoline–chalcone hybrids have been synthesized using a three-step pathway starting with Friedländer cyclocondensation between (2-aminophenyl)chalcones and acetone to give 2-methyl-4-styrylquinolines, followed by selective oxidation to the 2-formyl analogues, and finally Claisen–Schmidt condensation between the formyl intermediates and 1-acetylnaphthalene. All intermediates and the final products have been fully characterized by IR and $^{1}H/^{13}C$ NMR spectroscopy, and by high-resolution mass spectrometry, and the three products have been characterized by single-crystal X-ray diffraction. The molecular conformations of (*E*)-3-{4-[(*E*)-2-phenylethenyl]-quinolin-2-yl}-1-(naphthalen-1-yl)prop-2-en-1-one, $C_{30}H_{21}NO$, (IVa), and (*E*)-3-{4-[(*E*)-2-(4-fluorophenyl)ethenyl]quinolin-2-yl}-1-(naphthalen-1-yl)prop-2-en-1-one, $C_{30}H_{20}FNO$, (IVb), are very similar. In each compound, the molecules are linked into a three-dimensional array by hydrogen bonds, of the C—H···O and C—H···N types in (IVa), and of the C—H···O and C—H···π types in (IVb), and by two independent π–π stacking interactions. By contrast, the conformation of the chalcone unit in (*E*)-3-{4-[(*E*)-2-(2-chlorophenyl)ethenyl]-quinolin-2-yl}-1-(naphthalen-1-yl)prop-2-en-1-one, $C_{30}H_{20}ClNO$, (IVc), differs from those in (IVa) and (IVb). There are only weak hydrogen bonds in the structure of (IVc), but a single rather weak π–π stacking interaction links the molecules into chains. Comparisons are made with some related structures.

1. Introduction

Styrylquinolines constitute an important group of quinoline derivatives with high medicinal value due to their broad spectrum of bioactivities (Musiol, 2020), finding therapeutic applications as potential anticancer (Gao *et al.*, 2018; Mrozek-Wilczkiewicz *et al.*, 2019), antifungal (Cieslik *et al.*, 2012), antileishmanial (Luczywo *et al.*, 2021) and antiretroviral (Mouscadet & Desmaële, 2010) agents.

Their syntheses have presented a challenge because of the need for harsh reaction conditions and/or expensive catalysts normally required to couple the styryl fragment to the quinoline nucleus (Alacid & Nájera, 2009; Chaudhari *et al.*, 2013; Dabiri *et al.*, 2008; Jamal *et al.*, 2016), although some alternative and versatile methodologies have been also described to overcome such obstacles (Satish *et al.*, 2019; Meléndez *et al.*, 2020).

Chalcones also represent an outstanding class of compounds occurring in diverse natural and synthetic products. Apart from their natural occurrence and synthetic usage, they also show a wide range of biological activities (Zhuang *et al.*,

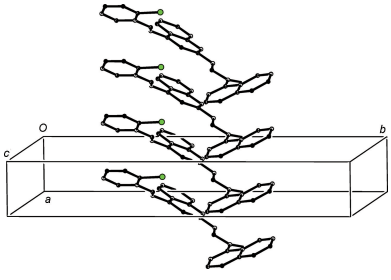

2017; Mohamed & Abuo-Rahma, 2020), in particular, their antibacterial (Xu *et al.*, 2019), anticolitic (Kim *et al.*, 2019), antifungal (Andrade *et al.*, 2018), antimalarial (Domínguez *et al.*, 2005), antioxidant (Vogel *et al.*, 2010) and antitumour (Sashidhara *et al.*, 2010; Ouyang *et al.*, 2021; Wang *et al.*, 2021) properties. Although several methods have been reported for the construction of the chalcone scaffold (Eddarir *et al.*, 2003; Reichwald *et al.*, 2008; Abbas Bukhari *et al.*, 2012), the base-catalyzed Claisen–Schmidt condensation is still the most convenient in terms of its simplicity and chemical versatility (Powers *et al.*, 1998).

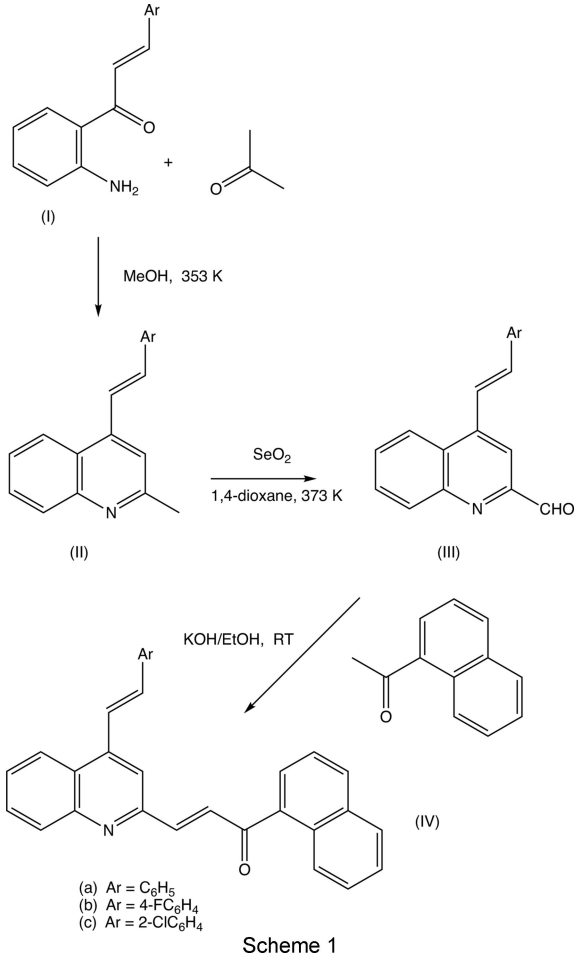

Scheme 1

In addition, it is well documented that the combination of the quinoline ring and the chalcone moiety into a single molecular entity results in promising molecular hybrids which are useful intermediates in the design and development of new potential multitarget drugs (Atukuri *et al.*, 2020; Mohamed & Abuo-Rahma, 2020). This class of conjugated compounds are known to possess remarkable antibacterial (Zheng *et al.*, 2011; Rao *et al.*, 2017), antifungal (Rao *et al.*, 2017), antimalarial (Domínguez *et al.*, 2005; Dave *et al.*, 2009), analgesic (Chabukswar *et al.*, 2016), anti-VIH (Chabukswar *et al.*, 2016) and anticancer (Kotra *et al.*, 2010; Mohamed & Abuo-Rahma, 2020) activities. The potential therapeutic properties of such compounds have prompted us to develop different methodologies to access this kind of molecular hybrid (de Carvalho Tavares *et al.*, 2011; Rosas-Sánchez *et al.*, 2015; Meléndez *et al.*, 2020; Mirzaei *et al.*, 2020).

We have recently used Friedländer annulation reactions to develop facile alternative routes for building novel compounds containing the 4-styrylquinoline framework, including some 4-styrylquinolinyl-3-chalcone hybrids, starting from (*E*)-1-(2-aminophenyl)-3-arylprop-2-en-1-ones of type (I) (see Scheme 1) (Meléndez *et al.*, 2020; Rodríguez *et al.*, 2020). In this work, we describe the application of the same methodology to the preparation of substituted 2-methyl-4-styrylquinolines (IIa)–(IIc) for use as precursors for the synthesis of the novel 4-styrylquinolinyl-2-chalcone molecular hybrids (IVa)–(IVc) in two further steps, involving first the selective oxidation of the 2-methyl group to give the 2-formyl intermediates (III), followed by Claisen–Schmidt condensation to give the target products (IV). We report here the synthesis, spectroscopic characterization and molecular and supramolecular structures of a matched set of three closely-related 4-styrylquinolinyl-2-chalcone hybrids, namely, (*E*)-1-(naphthalen-1-yl)-3-{4-[(*E*)-2-phenylethenyl]quinolin-2-yl}prop-2-en-1-one, (IVa), (*E*)-3-{4-[(*E*)-2-(4-fluorophenyl)ethenyl]quinolin-2-yl}-1-(naphthalen-1-yl)prop-2-en-1-one, (IVb), and (*E*)-3-{4-[(*E*)-2-(2-chlorophenyl)ethenyl]quinolin-2-yl}-1-(naphthalen-1-yl)prop-2-en-1-one, (IVc) (Scheme 1 and Figs. 1–3), which differ only in the nature of the substituents at positions C2 and C4 in the styryl fragment.

2. Experimental

2.1. Synthesis and crystallization

Compounds (IIa) and (IIc) were prepared using the procedure recently described by Vera *et al.* (2022) for the synthesis of compound (IIb).

Compound (IIa): reaction time 15 h, yield 0.19 g (86%), yellow solid, m.p. 367–369 K, R_F = 0.20 (12.5% ethyl acetate–hexane). Compound (IIc): reaction time 14 h, yield 0.21 g (73%), yellow solid, m.p. 388–390 K, R_F = 0.22 (12.5% ethyl acetate–hexane).

For the synthesis of compounds (III), a suspension of the appropriate 2-methyl-4-styrylquinoline (II) (1.0 mmol) and selenium dioxide (2.0 mmol) in 1,4-dioxane (5 ml) was stirred and heated at 373 K for the appropriate time. After the complete consumption of (II) [as monitored by thin-layer chromatography (TLC)], dichloromethane (15 ml) was added and the residual solid was removed by filtration. The solvent was removed under reduced pressure and the resulting crude products were purified by flash column chromatography on silica gel using hexane–ethyl acetate mixtures as eluent (compositions ranged from 7:1 to 2:1 *v*/*v*) to give the required formyl intermediates (IIIa)–(IIIc) as solid compounds.

Compound (IIIa): reaction time, 1 h, yield 0.23 g (96%), yellow solid, m.p. 421–423 K, R_F = 0.31 (9.1% ethyl acetate–hexane). Compound (IIIb): reaction time, 1 h, yield 0.14 g (89%), yellow solid, m.p. 417–419 K, R_F = 0.20 (9.1% ethyl acetate–hexane). Compound (IIIc): reaction time, 2 h, yield

0.21 g (92%), pale orange solid, m.p. 431–433 K, R_F = 0.28 (9.1% ethyl acetate–hexane).

For the synthesis of compounds (IV), a mixture of the appropriate 2-formyl intermediate (III) (1.0 mmol), 1-acetonaphthone (1.0 mmol) and potassium hydroxide (1.1 mmol) in ethanol (3 ml) was stirred at 298 K for the appropriate time. After complete consumption of (III) (monitored by TLC), the resulting precipitate was collected by filtration, washed with water (15 ml) and ethanol (10 ml), and then recrystallized from chloroform–ethanol to afford the target molecular hybrids (IV).

Compound (IVa): reaction time, 3 h, yield 0.13 g (82%), yellow solid, m.p. 450–452 K, R_F = 0.22 (13% ethyl acetate–hexane). Compound (IVb): reaction time, 2 h, yield 0.13 g (81%), yellow solid, m.p. 451–453 K, R_F = 0.31 (13% ethyl acetate–hexane). Compound (IVc): reaction time, 1 h, yield 0.14 g (95%), yellow solid, m.p. 441–443 K, R_F = 0.20 (9% ethyl acetate–hexane).

Full details of the spectroscopic characterization are included in the supporting information.

2.2. Refinement

Crystal data, data collection and refinement details for compounds (IVa)–(IVc) are summarized in Table 1. Two bad outlier reflections ($\bar{1}24$ and $\bar{3},\bar{6},12$) were omitted from the data set for compound (IVb). All H atoms were located in difference maps and then treated as riding atoms in geometrically idealized positions, with C—H distances of 0.95 Å and U_{iso}(H) = 1.2U_{eq}(C).

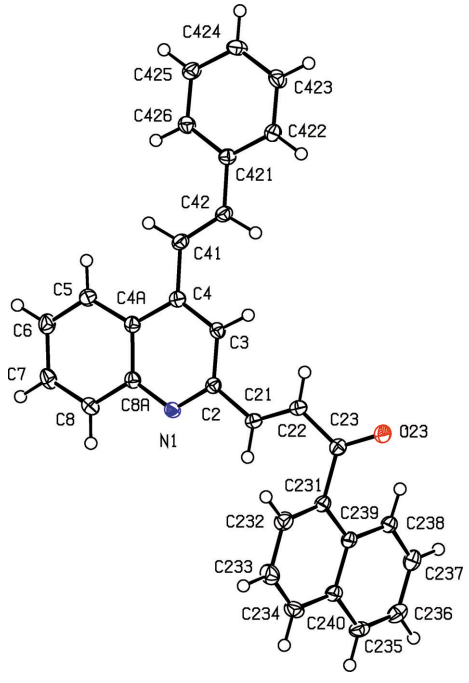

Figure 1
The molecular structure of compound (IVa), showing the atom-labelling scheme. Displacement ellipsoids are drawn at the 50% probability level.

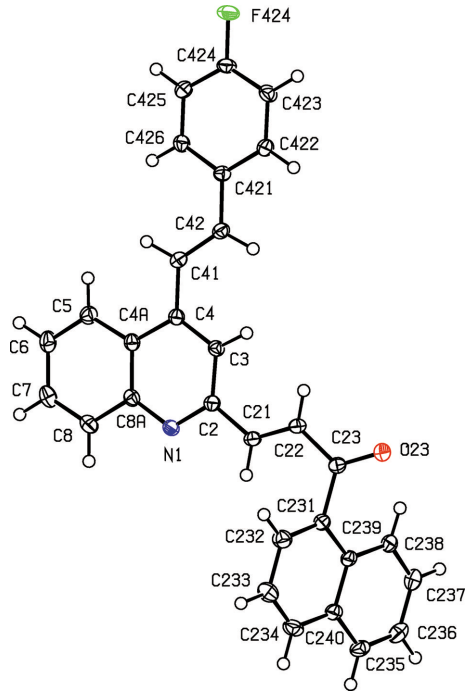

Figure 2
The molecular structure of compound (IVb), showing the atom-labelling scheme. Displacement ellipsoids are drawn at the 50% probability level.

3. Results and discussion

We have recently reported (Vera *et al.*, 2022) a high-yield synthesis of the 2-methyl-4-styrylquinoline (IIb) using the Friedländer cyclocondensation between the chalcone (Ib) (see Scheme 1) and acetone, along with its spectroscopic and crystallographic characterization. Using the same methodology, we have now prepared the corresponding styrylquinolines (IIa) and (IIc) in yields of 86 and 73%, respectively. All of the precursors (IIa)–(IIc) underwent selective oxidation with selenium dioxide to give the corresponding 2-formyl intermediates (IIIa)–(IIIc) with yields in the range 89–96% (see Section 2.1). Finally, Claisen–Schmidt condensation in the intermediates (III) with 1-acetonaphthone (1-acetylnaphthalene) gave the target hybrid products (IV) with yields in the range 81–95%. Compounds (IIa), (IIc), (IIIa)–(IIIc) and (IVa)–(IVc) were all fully characterized by FT–IR and ^{1}H/^{13}C NMR spectroscopy, and by high-resolution mass spectrometry (HRMS); full details of the spectroscopic characterization are provided in the supporting information.

The main spectroscopic features for the precursors (IIa) and (IIc) matched perfectly those of previously reported analogues (Vera *et al.*, 2022). The IR spectra of the formyl intermediates (III) showed the characteristic absorption band for the C=O group at 1699–1708 cm^{-1}, and their ^{1}H and ^{13}C NMR spectra contained the corresponding signals for the formyl group in the ranges δ 10.24–10.25 and 194.1–194.2, respectively.

The presence of stretching vibration bands in the range 1727–1731 cm^{-1}, attributed to a conjugated carbonyl group, are the salient features in the IR spectra of compounds

Table 1
Experimental details.

	(IVa)	(IVb)	(IVc)
Crystal data			
Chemical formula	$C_{30}H_{21}NO$	$C_{30}H_{20}FNO$	$C_{30}H_{20}ClNO$
M_r	411.48	429.47	445.92
Crystal system, space group	Triclinic, $P\overline{1}$	Triclinic, $P\overline{1}$	Monoclinic, $P2_1/c$
Temperature (K)	100	100	100
a, b, c (Å)	9.6151 (4), 10.0235 (4), 12.6299 (5)	9.6679 (12), 10.1279 (12), 12.6482 (13)	3.9184 (1), 24.6546 (8), 21.8833 (6)
α, β, γ (°)	67.766 (1), 71.191 (1), 84.004 (2)	111.420 (4), 103.871 (4), 96.632 (5)	90, 91.271 (1), 90
V (Å^3)	1066.34 (8)	1090.7 (2)	2113.55 (10)
Z	2	2	4
Radiation type	Mo $K\alpha$	Mo $K\alpha$	Mo $K\alpha$
μ (mm^{-1})	0.08	0.09	0.21
Crystal size (mm)	0.12 × 0.10 × 0.05	0.17 × 0.14 × 0.10	0.22 × 0.19 × 0.04
Data collection			
Diffractometer	Bruker D8 Venture	Bruker D8 Venture	Bruker D8 Venture
Absorption correction	Multi-scan (*SADABS*; Bruker, 2016)	Multi-scan (*SADABS*; Bruker, 2016)	Multi-scan (*SADABS*; Bruker, 2016)
T_{min}, T_{max}	0.928, 0.996	0.953, 0.992	0.912, 0.992
No. of measured, independent and observed [$I > 2\sigma(I)$] reflections	34856, 4719, 3964	47863, 5431, 4465	67339, 5301, 4855
R_{int}	0.052	0.057	0.049
(sin $\theta/\lambda)_{max}$ (Å^{-1})	0.642	0.668	0.670
Refinement			
$R[F^2 > 2\sigma(F^2)]$, $wR(F^2)$, S	0.042, 0.107, 1.03	0.044, 0.111, 1.04	0.046, 0.108, 1.16
No. of reflections	4719	5431	5301
No. of parameters	289	298	298
H-atom treatment	H-atom parameters constrained	H-atom parameters constrained	H-atom parameters constrained
$\Delta\rho_{max}$, $\Delta\rho_{min}$ (e Å^{-3})	0.28, −0.23	0.35, −0.25	0.40, −0.30

Computer programs: *APEX3* (Bruker, 2018), *SAINT* (Bruker, 2017), *SHELXT2014* (Sheldrick, 2015*a*), *SHELXL2014* (Sheldrick, 2015*b*) and *PLATON* (Spek, 2020).

(IVa)–(IVc). The formation of molecular hybrids (IV) was established by disappearance of the formyl signals from both the ^{1}H and ^{13}C NMR spectra, and by the appearance of signals from the newly formed 3-arylpropen-1-one fragment. As far as the Claisen–Schmidt condensation is concerned, it proceeded in a highly stereoselective manner, giving exclusively the *E*-stereoisomers, as indicated by the ^{1}H NMR spectra. The *trans* configuration of the arylpropen-1-one fragment was deduced on the basis of the coupling constant values ($^3J_{HA,HB}$ = 15.9 Hz) between H_A and H_B (α,β-enonic H atoms), whose signals in the ^{1}H NMR spectra appear at δ 7.91–7.93 and 7.78–7.79, respectively.

We also report here the molecular and supramolecular structures of the hybrid products (IVa)–(IVc) which fully confirm the molecular structures deduced from the spectroscopic data, in particular, the *E*-configuration of both the styryl and the chalcone moieties (Figs. 1–3). This synthetic pathway (see Scheme 1) is extremely versatile, in that it permits the introduction of substituents in both rings of the quinoline portion (*cf.* Rodríguez *et al.*, 2020), as well as in the styryl component (Vera *et al.*, 2022), while the Claisen–Schmidt reaction step introduces a very wide range of synthetic options. In addition, the presence of the chalcone unit in the compounds of type (IV) provides scope for an extensive variety of further synthetic elaborations utilizing this fragment (Powers *et al.*, 1998; Mohamed & Abuo-Rahma, 2020).

For each of (IVa)–(IVc), the atom labelling (Figs. 1–3) follows that employed in recent reports on styrylquinoline derivatives (Vera *et al.*, 2022; Ardila *et al.*, 2022). Compounds (IVa) and (IVb) are both triclinic (Table 1), and their corresponding unit-cell repeat distances are fairly similar; however, these compounds are not isomorphous, as the inter-axial angles in (IVa) are all less than 90°, whereas those in (IVb) are all greater than 90°. Moreover, the correponding pairs of angles are not supplementary, especially the β angle. By

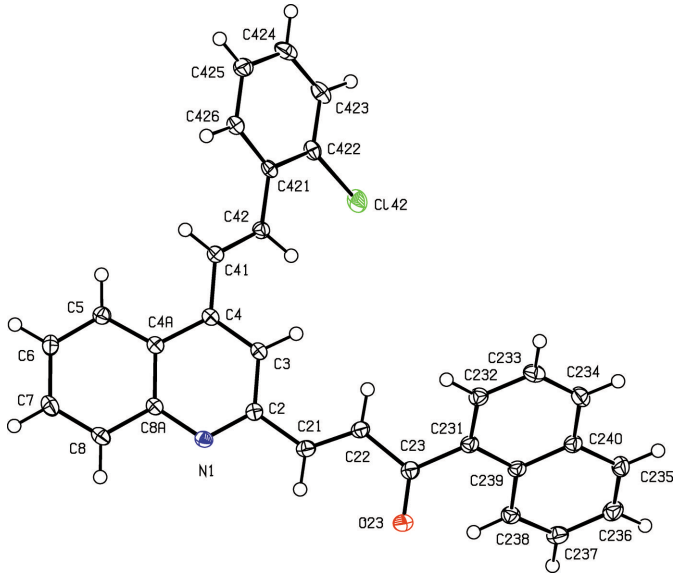

Figure 3
The molecular structure of compound (IVc), showing the atom-labelling scheme. Displacement ellipsoids are drawn at the 50% probability level.

Table 2
Selected torsion angles (°) for compounds (IVa)–(IVc).

Parameter	(IVa)	(IVb)	(IVc)
N1—C2—C21—C22	−178.23)12)	−178.25 (12)	−178.04 (14)
C21—C22—C23—O23	163.64 (12)	162.97 (12)	−1.9 (2)
C21—C22—C23—C231	−14.95 (19)	−15.59 (18)	169.99 (14)
C22—C23—C231—C232	−61.76 (17)	−59.28 (16)	41.01 (19)
C3—C4—C41—C42	16.1 (2)	16.2 (2)	27.2 (2)
C41—C42—C421—C422	166.57 (13)	165.01 (13)	−165.79 (15)

contrast, the crystals of (IVc) are monoclinic. None of the molecules in the products (IV) exhibits any internal symmetry, so that they are all conformationally chiral (Moss, 1996; Flack & Bernardinelli, 1999); the centrosymmetric space groups (Table 1) confirm that equal numbers of the two conformational enantiomers are present in each case. For each of (IVa)–(IVc), the reference molecule was selected as one having a positive sign for the torsion angle C3—C4—C41—C42 (Table 2). Overall the molecular conformations of (IVa) and (IVb) are quite similar, but that for (IVc) shows a marked difference in the orientation of the acyl fragment relative to the rest of the molecule, corresponding to a rotation of *ca* 180° around the C22—C23 bond (Table 2 and Figs. 1–3).

The supramolecular assembly in compound (IVa) is three-dimensional and it dependes upon a combination of C—H···O and C—H···N hydrogen bonds (Table 3), and two

Table 3
Hydrogen bonds and short intermolecular contacts (Å, °) for compounds (IVa)–(IVc).

*Cg*1 and *Cg*2 represent the centroids of the C231–C234/C240/C239 and C421–C426 rings, respectively.

Compound	*D*—H···*A*	*D*—H	H···*A*	*D*···*A*	*D*—H···*A*
(IVa)	C22—H22···O23^{i}	0.95	2.57	3.5183 (17)	177
	C234—H234···N1^{ii}	0.95	2.60	3.4207 (17)	145
	C422—H422···*Cg*1^{i}	0.95	2.93	3.7418 (16)	144
(IVb)	C22—H22···O23^{i}	0.95	2.59	3.5407 (17)	176
	C234—H234···N1^{iii}	0.95	2.67	3.5645 (18)	157
	C233—H233···*Cg*2^{iv}	0.95	2.85	3.6466 (18)	142
(IVc)	C8—H8···N1^{ii}	0.95	2.63	3.551 (2)	163
	C425—H425···O23^{v}	0.95	2.55	3.290 (2)	134

Symmetry codes: (i) $-x, -y+, -z+1$; (ii) $-x+1, -y+1, -z$; (iii) $-x+1, -y+2, -z+2$; (iv) $x, y+1, z+1$; (v) $-x+1, y-\frac{1}{2}, -z+\frac{1}{2}$.

different π–π stacking interactions. The formation of the three-dimensional framework structure is readily analysed in terms of three one-dimensional substructures (Ferguson *et al.*, 1998*a*,*b*; Gregson *et al.*, 2000), which, in the interests of clarity and simplicity, are illustrated separately. Inversion-related pairs of molecules are linked by almost linear C—H···O hydrogen bonds to form cyclic centrosymmetric dimers containing an $R_2^2(8)$ (Etter, 1990; Etter *et al.*, 1990; Bernstein *et al.*, 1995) ring, and this dimeric unit can be regarded as the basic building block in the overall structure.

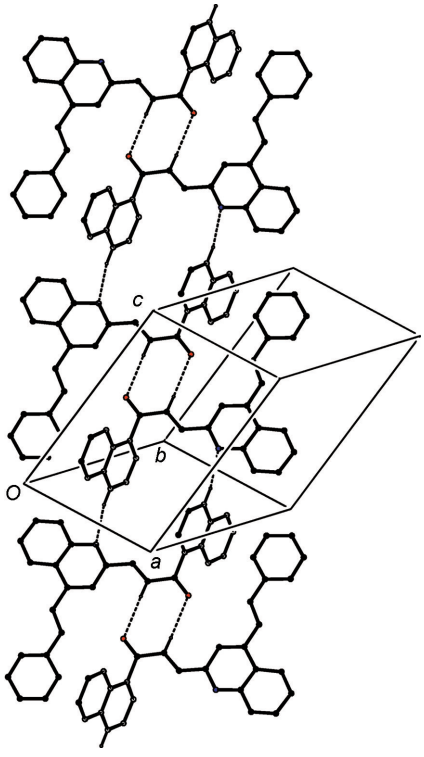

Figure 4
Part of the crystal structure of compound (IVa), showing the formation of a ribbon of alternating $R_2^2(8)$ and $R_2^2(20)$ rings running parallel to $[10\bar{1}]$. Hydrogen bonds are drawn as dashed lines and, for the sake of clarity, H atoms not involved in the motif shown have been omitted.

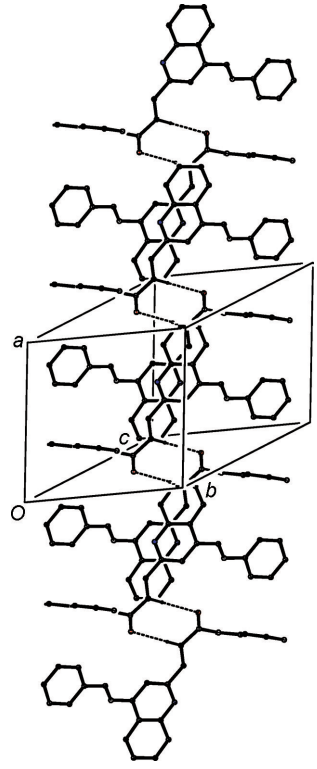

Figure 5
Part of the crystal structure of compound (IVa), showing the linking of the $R_2^2(8)$ dimers by a π-stacking interaction between pyridine rings, so forming a chain along [100]. Hydrogen bonds are drawn as dashed lines and, for the sake of clarity, H atoms not involved in the motif shown have been omitted.

The linking of these dimeric units by C—H···N hydrogen bonds gives rise to a ribbon running parallel to the [10$\bar{1}$] direction (Fig. 4), in which $R_2^2(8)$ rings centred at (n, $\frac{1}{2}$, $\frac{1}{2} - n$) alternate with $R_2^2(20)$ rings centred at ($\frac{1}{2} + n$, $\frac{1}{2}$, $-n$), where n represents an integer in each case. The pyridine rings of the molecules at (x, y, z) and ($-x + 1$, $-y + 1$, $-z + 1$) are strictly parallel with an interplanar spacing of 3.2877 (5) Å and a ring-centroid separation of 3.5372 (7) Å, corresponding to a ring-centroid offset of 1.305 (2) Å. This interaction links the $R_2^2(8)$ dimers to generate a second chain, this time running parallel to the [100] direction (Fig. 5). In the final substructure, the carbocyclic ring of the quinoline unit at (x, y, z) and the styryl ring at ($-x + 1$, $-y + 2$, $-z + 1$) make an interplanar angle of only 6.37 (7)°; the ring-centroid separation is 3.7818 (9) Å and the shortest perpendicular distance between the centroid of one ring and the plane of the other is 3.4535 (6) Å, corresponding to a ring-centroid offset of 1.541 (2) Å. This interaction links the $R_2^2(8)$ dimers into a chain running parallel to the [110] direction (Fig. 6), and the combination of chains along [100], [110] and [10$\bar{1}$] generates a three-dimensional structure.

The supramolecular assembly in compound (IVb) is also three-dimensional, built from a combination of C—H···O and C—H···π hydrogen bonds, and two π–π stacking interactions; the short intermolecular C—H···N contact in (IVb) (Table 3) is probably not structurally significant, as the H···N distance is only a little less than the sum, 2.70 Å, of the van der Waals radii (Rowland & Taylor, 1996). As in (IVa), the formation of the three-dimensional structure in (IVb) can be analysed in terms of three one-dimensional substructures, based on the linking of the $R_2^2(8)$ dimers formed by the C—H···O hydrogen bonds (Table 3). The linking of the $R_2^2(8)$ dimers by the C—H···π hydrogen bonds gives rise to a chain of rings running parallel to the [011] direction (Fig. 7) in which the $R_2^2(8)$ rings are centred at (0, $\frac{1}{2} + n$, $\frac{1}{2} + n$), and they alternate with the rings formed by C—H···π hydrogen bonds which are centred at (0, n, n), where n represents an integer in each case.

The two substructures formed by the π–π stacking interactions are entirely analogous to those formed in (IVa), such that they need no separate illustration. The pyridine rings at (x, y, z) and ($-x + 1$, $-y + 1$, $-z + 1$) in (IVb) have a ring-centroid offset of 1.319 (2) Å, and the carbocyclic ring of the quinoline unit at (x, y, z) and the styryl ring at ($-x + 1$, $-y$, $-z + 1$), which make an interplanar angle of only 2.38 (7)°, have a centroid offset of *ca* 1.576 (4) Å. These two interactions generate chains of π-stacked dimers running parallel to the [100] and [1$\bar{1}$0] directions, respectively. The combination of chains along [011], [100] and [1$\bar{1}$0] suffices to generate a three-dimensional assembly.

The direction-specific intermolecular interactions in the structure of (IVc) are all weak. There are C—H···N contacts between inversion-related pairs of molecules (Table 3); although these are almost linear, the H···N and C···N distances are long for hydrogen bonds and, indeed, *checkCIF* (Spek, 2020; https://checkcif.iucr.org/) raises a mild alert on these grounds. These contacts are perhaps best regarded as

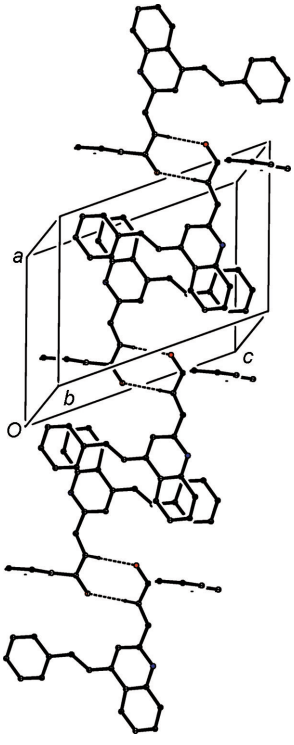

Figure 6
Part of the crystal structure of compound (IVa), showing the linking of the $R_2^2(8)$ dimers by a π-stacking interaction between carbocyclic rings, so forming a chain along [110]. Hydrogen bonds are drawn as dashed lines and, for the sake of clarity, H atoms not involved in the motif shown have been omitted.

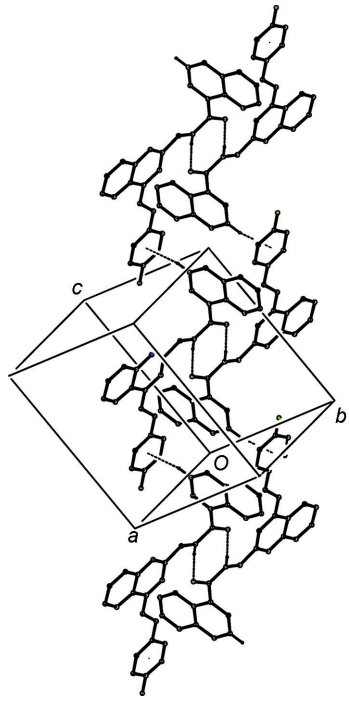

Figure 7
Part of the crystal structure of compound (IVb), showing the formation of a chain of centrosymmetric rings running parallel to the [011] direction. Hydrogen bonds are drawn as dashed lines and, for the sake of clarity, H atoms not involved in the motif shown have been omitted.

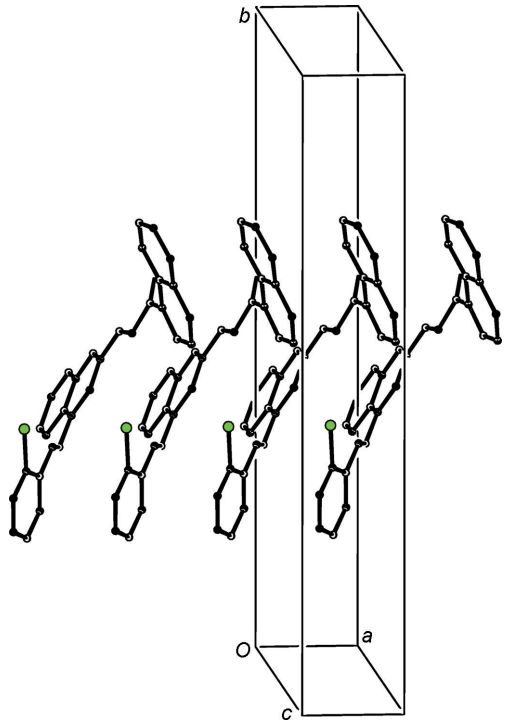

Figure 9
Part of the crystal structure of compound (IVc), showing the formation of a π-stacked chain along [100]. For the sake of clarity, H atoms have all been omitted.

being close to the margin of structural significance, but they serve to link the molecules into cyclic centrosymmetric $R_2^2(8)$ dimers (Fig. 8). On the other hand, the short intermolecular C—H···O contact (Table 3) has a very small D—H···A angle, such that the associated interaction is probably negligible (Wood *et al.*, 2009). In addition, molecules of (IVc) which are related by translation along [100] are stacked in register and for the ring containing atom C231 (Fig. 3), the interplanar spacing is 3.5843 (6) Å, associated with a ring-centroid separation of 3.9184 (9) Å and a ring-centroid offset of 1.584 (2) Å. This interaction provides a weak link between

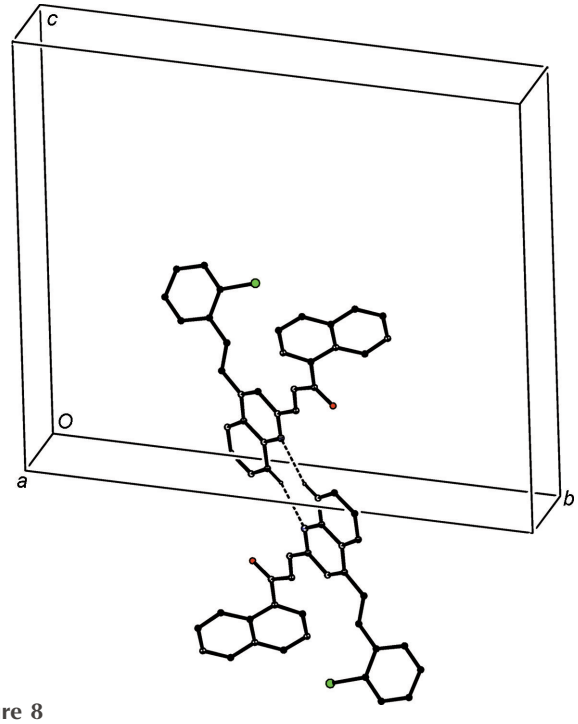

Figure 8
Part of the crystal structure of compound (IVc), showing the formation of a cyclic centrosymmetric dimer. Hydrogen bonds are drawn as dashed lines and, for the sake of clarity, H atoms not involved in the motif shown have been omitted.

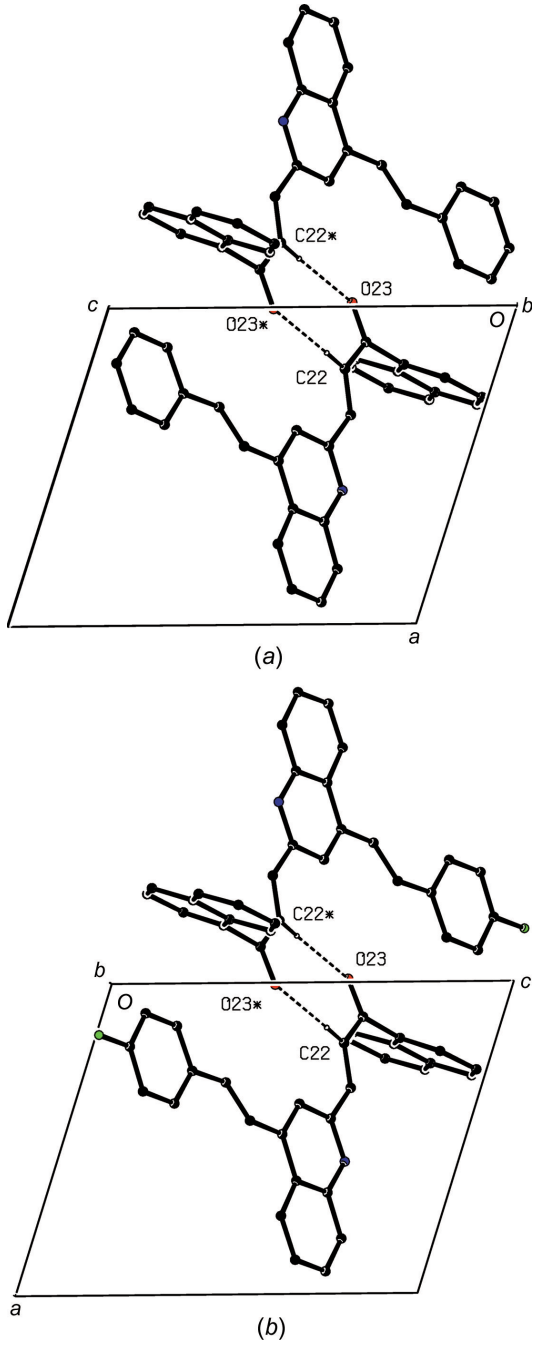

Figure 10
Projections along [010] of the cyclic dimers in (*a*) compound (IVa) and (*b*) compound (IVb). Hydrogen bonds are drawn as dashed lines and, for the sake of clarity, H atoms not involved in the motifs shown have been omitted. The atoms marked with an asterisk (*) are at the symmetry position ($-x$, $-y+1$, $-z+1$). Note the different locations of the origin and the different orientations of the axes.

adjacent molecules, forming a chain running parallel to the [100] direction (Fig. 9), leading overall to a stack of weakly hydrogen-bonded dimers.

It is interesting to note the structural contrasts between compounds (IVa) and (IVb) on the one hand, and compound (IVc) on the other, in terms of their space groups (Table 1), their molecular conformations (Table 2 and Figs. 1–3), the range of direction-specific intermolecular interactions and their modes of supramolecular assembly, as discussed above. All these points are associated with a change in the identity and location of a single monoatomic substituent in the styryl unit, but it is not easy to determine whether any one of these factors could be regarded as a possible cause of the effects observed in any, or all, of the others. Although the two triclinic compounds (IVa) and (IVb) have different inter-axial angles (Table 1) and different modes of supramolecular assembly, in both, the assembly is based on a cyclic centrosymmetric $R_2^2(8)$ dimer built from C—H···O hydrogen bonds (Table 3). It is thus striking that projections of the dimers in (IVa) and (IVb), viewed along [010], are extremely similar (Fig. 10), despite the different locations of the origin and the different orientations of the axes.

We have recently reported (Vera *et al.*, 2022) the structures of a number of 2-methyl-4-styrylquinolines of type (II) (see Scheme 1; all prepared using Friedländer cyclocondensation reactions, as here). In each of (*E*)-4-(4-fluorostyryl)-2-methylquinoline and (*E*)-2-methyl-4-[4-(trifluoromethyl)styryl]quinoline, the molecules are linked into cyclic centrosymmetric dimers by hydrogen bonds, of the C—H···N and C—H···π types, respectively, and these dimers are further linked by π–π stacking interactions to form sheets in the fluoro compound and chains in the trifluoromethyl analogue. By contrast, there are no significant intermolecular interactions in the structure of (*E*)-4-(2,6-dichlorostyryl)-2-methylquinoline. All of these type (II) compounds have molecular skeletons in which the styryl and quinoline units are non-coplanar, as reported here for compounds (IVa)–(IVc). This appears to be the case for all of the 4-styrylquinolines which have been structurally characterized so far, in contrast to the 2- and 8-styrylquinolines, where the two ring systems appear always to be effectively coplanar (Vera *et al.*, 2022; Ardila *et al.*, 2022).

4. Summary

We have developed a highly versatile and efficient three-step synthesis of a novel class of styrylquinoline–chalcone hybrids based on only very simple and readily available starting materials, such as simple aldehydes and ketones, and we have characterized by spectroscopic means (IR, ^{1}H/^{13}C NMR and HRMS) three products and all of the intermediates on the pathways leading to them, and we have determined the molecular and supramolecular structures of the three products.

Acknowledgements

JC and ID thank the Centro de Instrumentación Científico-Técnica of the Universidad de Jaén (UJA) and its staff for the data collection. AP is grateful for support from Vicerrectoría de Investigación y Extensión of the Industrial University of Santander. JC thanks the Universidad de Jaén and the Consejería de Economía, Innovación, Ciencia y Empleo (Junta de Andalucá, Spain) for financial support. ID also thanks Vicerrectoría de Investigación of Universidad de Jaén for a PhD Scholar fellowship.

Funding information

Funding for this research was provided by: Vicerrectoría de Investigación y Extensión of the Industrial University of Santander (grant No. 2680).

References

Abbas Bukhari, S. N., Jasamal, M. & Jantan, I. (2012). *Mini Rev. Med. Chem.* **12**, 394–1403.
Alacid, E. & Nájera, C. (2009). *J. Org. Chem.* **74**, 8191–8195.
Andrade, J. T., Santos, F. R. S., Lima, W. G., Sousa, C. D. F., Oliveira, L. S. F. M., Ribeiro, R. I. M. A., Gomes, A. J. P. S., Araújo, M. G. F., Villar, J. A. F. P. & Ferreira, J. M. S. (2018). *J. Antibiot.* **71**, 702–712.
Ardila, D. M., Rodríguez, D. F., Palma, A., Díaz Costa, I., Cobo, J. & Glidewell, C. (2022). *Acta Cryst.* C**78**, 671–680.
Atukuri, D., Vijayalaxmi, S., Sanjeevamurthy, R., Vidya, L., Prasannakumar, R. & Raghavendra, M. M. (2020). *Bioorg. Chem.* **105**, 104419.
Bernstein, J., Davis, R. E., Shimoni, L. & Chang, N.-L. (1995). *Angew. Chem. Int. Ed. Engl.* **34**, 1555–1573.
Bruker (2016). *SADABS*. Bruker AXS Inc., Madison, Wisconsin, USA.
Bruker (2017). *SAINT*. Bruker AXS Inc., Madison, Wisconsin, USA.
Bruker (2018). *APEX3*. Bruker AXS Inc., Madison, Wisconsin, USA.
Carvalho Tavares, L. de, Johann, S., Maria de Almeida Alves, T., Guerra, J. C., Maria de Souza-Fagundes, E., Cisalpino, P. S., Bortoluzzi, A. J., Caramori, G. F., de Mattos Piccoli, R., Braibante, H. T. S., Braibante, M. E. F. & Pizzolatti, M. G. (2011). *Eur. J. Med. Chem.* **46**, 4448–4456.
Chaudhari, C., Hakim Siddiki, S. M. A. & Shimizu, K. I. (2013). *Tetrahedron Lett.* **54**, 6490–6493.
Chabukswar, A. R., Kuchekar, B. S., Jagdale, S. C., Lokhande, P. D., Chabukswar, V. V., Shisodia, S. U., Mahabal, R. H., Londhe, A. M. & Ojha, N. S. (2016). *Arabian Journal of Chemistry*, **9**, 704–712.
Cieslik, W., Musiol, R., Nycz, J. E., Jampilek, J., Vejsova, M., Wolff, M., Machura, B. & Polanski, J. (2012). *Bioorg. Med. Chem.* **20**, 6960–6968.
Dabiri, M., Salehi, P., Baghbanzadeh, M. & Nikcheh, M. S. (2008). *Tetrahedron Lett.* **49**, 5366–5368.
Dave, S. S., Ghatole, A. M., Rahatgaonkar, A. M., Chorghade, M. S., Chauhan, P. & Srivastava, K. (2009). *Indian J. Chem. Sect. B*, **48**, 1780–1793.
Domínguez, J. N., León, C., Rodrigues, J., Gamboa de Domínguez, N., Gut, J. & Rosenthal, P. J. (2005). *J. Med. Chem.* **48**, 3654–3658.
Eddarir, S., Cotelle, N., Bakkour, Y. & Rolando, C. (2003). *Tetrahedron Lett.* **44**, 5359–5363.
Etter, M. C. (1990). *Acc. Chem. Res.* **23**, 120–126.
Etter, M. C., MacDonald, J. C. & Bernstein, J. (1990). *Acta Cryst.* B**46**, 256–262.
Ferguson, G., Glidewell, C., Gregson, R. M. & Meehan, P. R. (1998*a*). *Acta Cryst.* B**54**, 129–138.
Ferguson, G., Glidewell, C., Gregson, R. M. & Meehan, P. R. (1998*b*). *Acta Cryst.* B**54**, 139–150.
Flack, H. D. & Bernardinelli, G. (1999). *Acta Cryst.* A**55**, 908–915.

Gao, W., Li, Z., Xu, Q. & Li, Y. (2018). *RSC Adv.* **8**, 38844–38849.
Gregson, R. M., Glidewell, C., Ferguson, G. & Lough, A. J. (2000). *Acta Cryst.* B**56**, 39–57.
Jamal, Z., Teo, Y.-C. & Lim, G. S. (2016). *Tetrahedron*, **72**, 2132–2138.
Kim, W., Lee, H., Kim, S., Joo, S., Jeong, S., Yoo, J. W. & Jung, Y. (2019). *Eur. J. Pharmacol.* **865**, 172722.
Kotra, V., Ganapaty, S. & Adapa, S. R. (2010). *Indian J. Chem. Sect. B*, **49**, 1109–1116.
Luczywo, A., Sauter, I. P., Silva Ferreira, T. C., Cortez, M., Romanelli, G. P., Sathicq, G. & Asís, S. E. (2021). *J. Heterocycl. Chem.* **58**, 822–832.
Meléndez, A., Plata, E., Rodríguez, D., Ardila, D., Guerrero, S., Acosta, L., Cobo, J., Nogueras, M. & Palma, A. (2020). *Synthesis*, **52**, 1804–1822.
Mirzaei, S., Hadizadeh, F., Eisvand, F., Mosaffa, F. & Ghodsi, R. (2020). *J. Mol. Struct.* **1202**, 127310.
Mohamed, M. F. A. & Abuo-Rahma, G. E. A. (2020). *RSC Adv.* **10**, 31139–31155.
Moss, G. P. (1996). *Pure Appl. Chem.* **68**, 2193–2222.
Mouscadet, J. F. & Desmaële, D. (2010). *Molecules*, **15**, 3048–3078.
Mrozek-Wilczkiewicz, A., Kuczak, M., Malarz, K., Cieślik, W., Spaczyńska, E. & Musiol, R. (2019). *Eur. J. Med. Chem.* **177**, 338–349.
Musiol, R. (2020). *Med. Chem.* **16**, 141–154.
Ouyang, Y., Li, J., Chen, X., Fu, X., Sun, S. & Wu, Q. (2021). *Biomolecules*, **11**, 1–36.
Powers, D. G., Casebier, D. S., Fokas, D., Ryan, W. J., Troth, J. R. & Coffen, D. L. (1998). *Tetrahedron*, **54**, 4085–4096.
Rao, N. S., Shaik, A. B., Routhu, S. R., Hussaini, S. M. A., Sunkari, S., Rao, A. V. S., Reddy, A. M., Alarifi, A. & Kamal, A. (2017). *ChemistrySelect*, **2**, 2989–2996.
Reichwald, C., Shimony, O., Sacerdoti-Sierra, N., Jaffe, C. L. & Kunick, C. (2008). *Bioorg. Med. Chem. Lett.* **18**, 1985–1989.
Rodríguez, D., Guerrero, S. A., Palma, A., Cobo, J. & Glidewell, C. (2020). *Acta Cryst.* C**76**, 883–890.
Rosas-Sánchez, A., Toscano, R. A., López-Cortés, J. G. & Ortega-Alfaro, M. C. (2015). *Dalton Trans.* **44**, 578–590.
Rowland, R. S. & Taylor, R. (1996). *J. Phys. Chem.* **100**, 7384–7391.
Sashidhara, K. V., Kumar, A., Kumar, M., Sarkar, J. & Sinha, S. (2010). *Bioorg. Med. Chem. Lett.* **20**, 7205–7211.
Satish, G., Ashok, P., Kota, L. & Ilangovan, A. (2019). *ChemistrySelect*, **4**, 1346–1349.
Sheldrick, G. M. (2015*a*). *Acta Cryst.* A**71**, 3–8.
Sheldrick, G. M. (2015*b*). *Acta Cryst.* C**71**, 3–8.
Spek, A. L. (2020). *Acta Cryst.* E**76**, 1–11.
Vera, D. R., Mantilla, J. P., Palma, A., Cobo, J. & Glidewell, C. (2022). *Acta Cryst.* C**78**, 524–530.
Vogel, S., Barbic, M., Jürgenliemk, G. & Heilmann, J. (2010). *Eur. J. Med. Chem.* **45**, 2206–2213.
Wang, K.-L., Yu, Y.-C. & Hsia, S.-M. (2021). *Cancers*, **13**, 115.
Wood, P. A., Allen, F. H. & Pidcock, E. (2009). *CrystEngComm*, **11**, 1563–1571.
Xu, M., Wu, P., Shen, F., Ji, J. & Rakesh, K. P. (2019). *Bioorg. Chem.* **91**, 103133.
Zheng, C. J., Jiang, S. M., Chen, Z. H., Ye, B. J. & Piao, H. R. (2011). *Arch. Pharm. Pharm. Med. Chem.* **344**, 689–695.
Zhuang, C., Zhang, W., Sheng, C., Zhang, W., Xing, C. & Miao, Z. (2017). *Chem. Rev.* **117**, 7762–7810.

supporting information

Acta Cryst. (2023). C**79**, 3-11 [https://doi.org/10.1107/S2053229622011263]

A three-step pathway from (2-aminophenyl)chalcones to novel styrylquinoline–chalcone hybrids: synthesis and spectroscopic and structural characterization of three examples

Diana R. Vera, Juan P. Mantilla, Alirio Palma, Iván Díaz Costa, Justo Cobo and Christopher Glidewell

Computing details

For all structures, data collection: *APEX3* (Bruker, 2018); cell refinement: *SAINT* (Bruker, 2017); data reduction: *SAINT* (Bruker, 2017); program(s) used to solve structure: SHELXT2014 (Sheldrick, 2015a); program(s) used to refine structure: *SHELXL2014* (Sheldrick, 2015b); molecular graphics: *PLATON* (Spek, 2020); software used to prepare material for publication: *SHELXL2014* (Sheldrick, 2015b) and *PLATON* (Spek, 2020).

((*E*)-1-(Naphthalen-1-yl)-3-{4-[(*E*)-2-phenylethenyl]quinolin-2-yl}-prop-2-en-1-one (IVa)

Crystal data

$C_{30}H_{21}NO$
$M_r = 411.48$
Triclinic, $P\overline{1}$
$a = 9.6151$ (4) Å
$b = 10.0235$ (4) Å
$c = 12.6299$ (5) Å
$\alpha = 67.766$ (1)°
$\beta = 71.191$ (1)°
$\gamma = 84.004$ (2)°
$V = 1066.34$ (8) Å^3
$Z = 2$
$F(000) = 432$
$D_x = 1.281$ Mg m^{-3}
Mo $K\alpha$ radiation, $\lambda = 0.71073$ Å
Cell parameters from 4719 reflections
$\theta = 2.2$–27.1°
$\mu = 0.08$ mm^{-1}
$T = 100$ K
Block, yellow
0.12 × 0.10 × 0.05 mm

Data collection

Bruker D8 Venture diffractometer
Radiation source: INCOATEC high brilliance microfocus sealed tube
Multilayer mirror monochromator
φ and ω scans
Absorption correction: multi-scan (SADABS; Bruker, 2016)
$T_{min} = 0.928$, $T_{max} = 0.996$
34856 measured reflections
4719 independent reflections
3964 reflections with $I > 2\sigma(I)$
$R_{int} = 0.052$
$\theta_{max} = 27.1°$, $\theta_{min} = 2.2°$
$h = -12 \rightarrow 12$
$k = -12 \rightarrow 12$
$l = -16 \rightarrow 16$

Refinement

Refinement on F^2
Least-squares matrix: full
$R[F^2 > 2\sigma(F^2)] = 0.042$
$wR(F^2) = 0.107$
$S = 1.03$
4719 reflections
289 parameters
0 restraints

Primary atom site location: dual
Hydrogen site location: inferred from neighbouring sites
H-atom parameters constrained

$w = 1/[\sigma^2(F_o^2) + (0.0422P)^2 + 0.5277P]$ where $P = (F_o^2 + 2F_c^2)/3$
$(\Delta/\sigma)_{max} < 0.001$
$\Delta\rho_{max} = 0.28$ e Å^{-3}
$\Delta\rho_{min} = -0.23$ e Å^{-3}

Special details

Geometry. All e.s.d.'s (except the e.s.d. in the dihedral angle between two l.s. planes) are estimated using the full covariance matrix. The cell e.s.d.'s are taken into account individually in the estimation of e.s.d.'s in distances, angles and torsion angles; correlations between e.s.d.'s in cell parameters are only used when they are defined by crystal symmetry. An approximate (isotropic) treatment of cell e.s.d.'s is used for estimating e.s.d.'s involving l.s. planes.

Fractional atomic coordinates and isotropic or equivalent isotropic displacement parameters (Å²)

	x	*y*	*z*	U_{iso}*/U_{eq}
N1	0.58182 (12)	0.60098 (11)	0.28402 (9)	0.0169 (2)
C2	0.44193 (13)	0.59239 (13)	0.35167 (11)	0.0161 (2)
C3	0.39095 (13)	0.65025 (13)	0.44327 (11)	0.0164 (2)
H3	0.2905	0.6383	0.4906	0.020*
C4	0.48623 (14)	0.72399 (13)	0.46437 (11)	0.0166 (3)
C4A	0.63712 (14)	0.73772 (13)	0.39112 (11)	0.0168 (3)
C5	0.74710 (14)	0.81174 (15)	0.40100 (12)	0.0208 (3)
H5	0.7211	0.8592	0.4569	0.025*
C6	0.89017 (15)	0.81614 (15)	0.33148 (12)	0.0237 (3)
H6	0.9620	0.8676	0.3387	0.028*
C7	0.93177 (15)	0.74485 (15)	0.24919 (12)	0.0238 (3)
H7	1.0319	0.7459	0.2031	0.029*
C8	0.82877 (14)	0.67416 (14)	0.23534 (12)	0.0213 (3)
H8	0.8576	0.6272	0.1791	0.026*
C8A	0.67913 (14)	0.67050 (13)	0.30442 (11)	0.0172 (3)
C21	0.34496 (14)	0.51785 (13)	0.32207 (11)	0.0171 (3)
H21	0.3905	0.4809	0.2603	0.020*
C22	0.19959 (14)	0.49592 (14)	0.37212 (11)	0.0188 (3)
H22	0.1486	0.5381	0.4294	0.023*
C23	0.11599 (14)	0.40842 (13)	0.34124 (11)	0.0183 (3)
O23	−0.00819 (10)	0.36329 (11)	0.40568 (9)	0.0240 (2)
C231	0.18810 (14)	0.37312 (14)	0.23051 (11)	0.0181 (3)
C232	0.22990 (16)	0.48266 (15)	0.11968 (12)	0.0236 (3)
H232	0.2162	0.5799	0.1145	0.028*
C233	0.29276 (16)	0.45308 (16)	0.01363 (12)	0.0269 (3)
H233	0.3186	0.5300	−0.0623	0.032*
C234	0.31646 (15)	0.31404 (16)	0.01998 (12)	0.0241 (3)
H234	0.3597	0.2949	−0.0517	0.029*
C235	0.30219 (14)	0.05256 (15)	0.14063 (13)	0.0227 (3)
H235	0.3452	0.0324	0.0693	0.027*
C236	0.26537 (15)	−0.05852 (15)	0.24908 (13)	0.0245 (3)
H236	0.2835	−0.1549	0.2528	0.029*
C237	0.20025 (15)	−0.03071 (15)	0.35601 (13)	0.0228 (3)
H237	0.1758	−0.1085	0.4314	0.027*

C238	0.17219 (14)	0.10791 (14)	0.35158 (12)	0.0182 (3)
H238	0.1266	0.1251	0.4240	0.022*
C239	0.21049 (13)	0.22633 (14)	0.23990 (11)	0.0170 (3)
C240	0.27737 (13)	0.19798 (14)	0.13227 (12)	0.0188 (3)
C41	0.43893 (14)	0.78369 (14)	0.55991 (11)	0.0188 (3)
H41	0.5020	0.8535	0.5560	0.023*
C42	0.31501 (14)	0.74817 (14)	0.65168 (11)	0.0190 (3)
H42	0.2497	0.6819	0.6534	0.023*
C421	0.27082 (14)	0.80271 (14)	0.75031 (11)	0.0177 (3)
C422	0.12552 (14)	0.78031 (14)	0.82574 (12)	0.0207 (3)
H422	0.0589	0.7283	0.8134	0.025*
C423	0.07723 (15)	0.83292 (15)	0.91825 (12)	0.0231 (3)
H423	−0.0221	0.8177	0.9681	0.028*
C424	0.17382 (15)	0.90764 (15)	0.93802 (12)	0.0233 (3)
H424	0.1408	0.9444	1.0009	0.028*
C425	0.31920 (15)	0.92837 (16)	0.86518 (12)	0.0237 (3)
H425	0.3859	0.9787	0.8790	0.028*
C426	0.36782 (14)	0.87625 (15)	0.77250 (12)	0.0211 (3)
H426	0.4677	0.8905	0.7237	0.025*

Atomic displacement parameters (Å²)

	U^{11}	U^{22}	U^{33}	U^{12}	U^{13}	U^{23}
N1	0.0182 (5)	0.0170 (5)	0.0148 (5)	0.0001 (4)	−0.0041 (4)	−0.0057 (4)
C2	0.0176 (6)	0.0142 (6)	0.0158 (6)	0.0001 (5)	−0.0056 (5)	−0.0043 (5)
C3	0.0150 (6)	0.0165 (6)	0.0164 (6)	0.0006 (5)	−0.0038 (5)	−0.0056 (5)
C4	0.0186 (6)	0.0154 (6)	0.0156 (6)	0.0012 (5)	−0.0063 (5)	−0.0048 (5)
C4A	0.0175 (6)	0.0170 (6)	0.0151 (6)	−0.0003 (5)	−0.0058 (5)	−0.0042 (5)
C5	0.0202 (6)	0.0254 (7)	0.0182 (6)	−0.0023 (5)	−0.0065 (5)	−0.0083 (5)
C6	0.0187 (6)	0.0291 (7)	0.0235 (7)	−0.0047 (5)	−0.0078 (5)	−0.0076 (6)
C7	0.0154 (6)	0.0297 (7)	0.0218 (7)	−0.0018 (5)	−0.0024 (5)	−0.0067 (6)
C8	0.0197 (6)	0.0235 (7)	0.0180 (6)	0.0005 (5)	−0.0024 (5)	−0.0076 (5)
C8A	0.0185 (6)	0.0163 (6)	0.0148 (6)	−0.0001 (5)	−0.0055 (5)	−0.0033 (5)
C21	0.0205 (6)	0.0156 (6)	0.0166 (6)	0.0013 (5)	−0.0065 (5)	−0.0071 (5)
C22	0.0205 (6)	0.0191 (6)	0.0192 (6)	0.0006 (5)	−0.0057 (5)	−0.0100 (5)
C23	0.0178 (6)	0.0171 (6)	0.0210 (6)	0.0015 (5)	−0.0070 (5)	−0.0075 (5)
O23	0.0173 (5)	0.0283 (5)	0.0287 (5)	−0.0028 (4)	−0.0030 (4)	−0.0153 (4)
C231	0.0164 (6)	0.0214 (6)	0.0196 (6)	−0.0010 (5)	−0.0073 (5)	−0.0091 (5)
C232	0.0278 (7)	0.0203 (6)	0.0235 (7)	−0.0006 (5)	−0.0094 (6)	−0.0074 (5)
C233	0.0304 (7)	0.0290 (7)	0.0175 (6)	−0.0032 (6)	−0.0073 (6)	−0.0034 (5)
C234	0.0231 (7)	0.0345 (8)	0.0174 (6)	−0.0002 (6)	−0.0062 (5)	−0.0121 (6)
C235	0.0179 (6)	0.0307 (7)	0.0289 (7)	0.0045 (5)	−0.0096 (5)	−0.0199 (6)
C236	0.0227 (7)	0.0221 (7)	0.0364 (8)	0.0045 (5)	−0.0141 (6)	−0.0157 (6)
C237	0.0213 (6)	0.0212 (6)	0.0269 (7)	−0.0008 (5)	−0.0115 (5)	−0.0061 (5)
C238	0.0151 (6)	0.0234 (6)	0.0196 (6)	−0.0005 (5)	−0.0073 (5)	−0.0097 (5)
C239	0.0129 (6)	0.0218 (6)	0.0200 (6)	−0.0003 (5)	−0.0073 (5)	−0.0097 (5)
C240	0.0146 (6)	0.0260 (7)	0.0212 (6)	0.0004 (5)	−0.0080 (5)	−0.0122 (5)
C41	0.0184 (6)	0.0198 (6)	0.0215 (6)	−0.0006 (5)	−0.0070 (5)	−0.0103 (5)

C42	0.0187 (6)	0.0209 (6)	0.0210 (6)	−0.0001 (5)	−0.0074 (5)	−0.0105 (5)
C421	0.0178 (6)	0.0189 (6)	0.0181 (6)	0.0018 (5)	−0.0069 (5)	−0.0077 (5)
C422	0.0179 (6)	0.0240 (7)	0.0222 (6)	−0.0016 (5)	−0.0062 (5)	−0.0102 (5)
C423	0.0163 (6)	0.0299 (7)	0.0225 (7)	0.0003 (5)	−0.0028 (5)	−0.0115 (6)
C424	0.0240 (7)	0.0296 (7)	0.0204 (6)	0.0032 (5)	−0.0061 (5)	−0.0149 (6)
C425	0.0207 (6)	0.0308 (7)	0.0259 (7)	−0.0016 (5)	−0.0083 (5)	−0.0156 (6)
C426	0.0160 (6)	0.0273 (7)	0.0217 (6)	−0.0005 (5)	−0.0044 (5)	−0.0118 (5)

Geometric parameters (Å, º)

N1—C2	1.3320 (16)	C233—H233	0.9500
N1—C8A	1.3619 (16)	C234—C240	1.4160 (19)
C2—C3	1.4134 (17)	C234—H234	0.9500
C2—C21	1.4660 (17)	C235—C236	1.363 (2)
C3—C4	1.3801 (17)	C235—C240	1.4212 (19)
C3—H3	0.9500	C235—H235	0.9500
C4—C4A	1.4351 (17)	C236—C237	1.4131 (19)
C4—C41	1.4685 (17)	C236—H236	0.9500
C4A—C5	1.4154 (18)	C237—C238	1.3708 (19)
C4A—C8A	1.4256 (17)	C237—H237	0.9500
C5—C6	1.3674 (18)	C238—C239	1.4225 (18)
C5—H5	0.9500	C238—H238	0.9500
C6—C7	1.409 (2)	C239—C240	1.4257 (17)
C6—H6	0.9500	C41—C42	1.3325 (18)
C7—C8	1.3659 (19)	C41—H41	0.9500
C7—H7	0.9500	C42—C421	1.4686 (17)
C8—C8A	1.4178 (17)	C42—H42	0.9500
C8—H8	0.9500	C421—C422	1.3983 (18)
C21—C22	1.3383 (18)	C421—C426	1.4001 (18)
C21—H21	0.9500	C422—C423	1.3871 (18)
C22—C23	1.4750 (17)	C422—H422	0.9500
C22—H22	0.9500	C423—C424	1.3865 (19)
C23—O23	1.2249 (16)	C423—H423	0.9500
C23—C231	1.5032 (17)	C424—C425	1.3893 (19)
C231—C232	1.3758 (18)	C424—H424	0.9500
C231—C239	1.4295 (18)	C425—C426	1.3858 (18)
C232—C233	1.4101 (19)	C425—H425	0.9500
C232—H232	0.9500	C426—H426	0.9500
C233—C234	1.364 (2)		

C2—N1—C8A	117.65 (10)	C233—C234—C240	120.75 (12)
N1—C2—C3	123.31 (11)	C233—C234—H234	119.6
N1—C2—C21	113.81 (11)	C240—C234—H234	119.6
C3—C2—C21	122.88 (11)	C236—C235—C240	121.18 (12)
C4—C3—C2	120.41 (11)	C236—C235—H235	119.4
C4—C3—H3	119.8	C240—C235—H235	119.4
C2—C3—H3	119.8	C235—C236—C237	120.20 (13)
C3—C4—C4A	117.54 (11)	C235—C236—H236	119.9

C3—C4—C41	122.35 (11)	C237—C236—H236	119.9
C4A—C4—C41	120.08 (11)	C238—C237—C236	120.38 (13)
C5—C4A—C8A	118.05 (11)	C238—C237—H237	119.8
C5—C4A—C4	124.07 (11)	C236—C237—H237	119.8
C8A—C4A—C4	117.87 (11)	C237—C238—C239	120.80 (12)
C6—C5—C4A	121.14 (12)	C237—C238—H238	119.6
C6—C5—H5	119.4	C239—C238—H238	119.6
C4A—C5—H5	119.4	C238—C239—C240	118.67 (12)
C5—C6—C7	120.44 (12)	C238—C239—C231	123.07 (11)
C5—C6—H6	119.8	C240—C239—C231	118.25 (12)
C7—C6—H6	119.8	C234—C240—C235	121.50 (12)
C8—C7—C6	120.33 (12)	C234—C240—C239	119.74 (12)
C8—C7—H7	119.8	C235—C240—C239	118.76 (12)
C6—C7—H7	119.8	C42—C41—C4	125.49 (12)
C7—C8—C8A	120.39 (12)	C42—C41—H41	117.3
C7—C8—H8	119.8	C4—C41—H41	117.3
C8A—C8—H8	119.8	C41—C42—C421	125.55 (12)
N1—C8A—C8	117.28 (11)	C41—C42—H42	117.2
N1—C8A—C4A	123.14 (11)	C421—C42—H42	117.2
C8—C8A—C4A	119.58 (12)	C422—C421—C426	118.32 (11)
C22—C21—C2	127.43 (11)	C422—C421—C42	118.74 (11)
C22—C21—H21	116.3	C426—C421—C42	122.94 (11)
C2—C21—H21	116.3	C423—C422—C421	121.01 (12)
C21—C22—C23	122.17 (11)	C423—C422—H422	119.5
C21—C22—H22	118.9	C421—C422—H422	119.5
C23—C22—H22	118.9	C424—C423—C422	120.07 (12)
O23—C23—C22	120.70 (11)	C424—C423—H423	120.0
O23—C23—C231	120.84 (11)	C422—C423—H423	120.0
C22—C23—C231	118.45 (11)	C423—C424—C425	119.54 (12)
C232—C231—C239	120.06 (12)	C423—C424—H424	120.2
C232—C231—C23	119.70 (12)	C425—C424—H424	120.2
C239—C231—C23	120.23 (11)	C426—C425—C424	120.57 (12)
C231—C232—C233	121.14 (13)	C426—C425—H425	119.7
C231—C232—H232	119.4	C424—C425—H425	119.7
C233—C232—H232	119.4	C425—C426—C421	120.47 (12)
C234—C233—C232	120.04 (13)	C425—C426—H426	119.8
C234—C233—H233	120.0	C421—C426—H426	119.8
C232—C233—H233	120.0		

C8A—N1—C2—C3	−0.63 (18)	C23—C231—C232—C233	−177.60 (12)
C8A—N1—C2—C21	179.07 (11)	C231—C232—C233—C234	−1.6 (2)
N1—C2—C3—C4	2.04 (19)	C232—C233—C234—C240	0.6 (2)
C21—C2—C3—C4	−177.63 (11)	C240—C235—C236—C237	0.5 (2)
C2—C3—C4—C4A	−0.60 (17)	C235—C236—C237—C238	0.7 (2)
C2—C3—C4—C41	−178.86 (11)	C236—C237—C238—C239	−1.23 (19)
C3—C4—C4A—C5	179.13 (12)	C237—C238—C239—C240	0.66 (18)
C41—C4—C4A—C5	−2.57 (19)	C237—C238—C239—C231	−177.90 (12)
C3—C4—C4A—C8A	−1.96 (17)	C232—C231—C239—C238	178.94 (12)

C41—C4—C4A—C8A	176.34 (11)	C23—C231—C239—C238	−2.34 (18)
C8A—C4A—C5—C6	−1.44 (19)	C232—C231—C239—C240	0.38 (18)
C4—C4A—C5—C6	177.46 (12)	C23—C231—C239—C240	179.10 (11)
C4A—C5—C6—C7	−0.9 (2)	C233—C234—C240—C235	−179.56 (13)
C5—C6—C7—C8	2.0 (2)	C233—C234—C240—C239	0.9 (2)
C6—C7—C8—C8A	−0.6 (2)	C236—C235—C240—C234	179.47 (12)
C2—N1—C8A—C8	177.54 (11)	C236—C235—C240—C239	−1.02 (19)
C2—N1—C8A—C4A	−2.19 (18)	C238—C239—C240—C234	179.98 (11)
C7—C8—C8A—N1	178.51 (12)	C231—C239—C240—C234	−1.40 (18)
C7—C8—C8A—C4A	−1.75 (19)	C238—C239—C240—C235	0.45 (17)
C5—C4A—C8A—N1	−177.52 (12)	C231—C239—C240—C235	179.07 (11)
C4—C4A—C8A—N1	3.50 (18)	C3—C4—C41—C42	16.1 (2)
C5—C4A—C8A—C8	2.75 (18)	C4A—C4—C41—C42	−162.09 (13)
C4—C4A—C8A—C8	−176.22 (11)	C4—C41—C42—C421	176.97 (12)
N1—C2—C21—C22	−178.23 (12)	C41—C42—C421—C422	166.57 (13)
C3—C2—C21—C22	1.5 (2)	C41—C42—C421—C426	−13.5 (2)
C2—C21—C22—C23	−174.78 (12)	C426—C421—C422—C423	1.8 (2)
C21—C22—C23—O23	163.64 (13)	C42—C421—C422—C423	−178.31 (12)
C21—C22—C23—C231	−14.95 (19)	C421—C422—C423—C424	−0.7 (2)
O23—C23—C231—C232	119.65 (15)	C422—C423—C424—C425	−0.5 (2)
C22—C23—C231—C232	−61.76 (17)	C423—C424—C425—C426	0.6 (2)
O23—C23—C231—C239	−59.07 (17)	C424—C425—C426—C421	0.5 (2)
C22—C23—C231—C239	119.52 (13)	C422—C421—C426—C425	−1.6 (2)
C239—C231—C232—C233	1.1 (2)	C42—C421—C426—C425	178.45 (13)

Hydrogen-bond geometry (Å, º)

D—H···*A*	*D*—H	H···*A*	*D*···*A*	*D*—H···*A*
C22—H22···O23^{i}	0.95	2.57	3.5183 (17)	177
C234—H234···N1^{ii}	0.95	2.60	3.4207 (17)	145
C422—H422···*Cg*1^{i}	0.95	2.93	3.7418 (16)	144

Symmetry codes: (i) −*x*, −*y*+1, −*z*+1; (ii) −*x*+1, −*y*+1, −*z*.

(*E*)-3-{4-[(*E*)-2-(4-Fluorophenyl)ethenyl]quinolin-2-yl}-1-(naphthalen-1-yl)prop-2-en-1-one (IVb)

Crystal data

$C_{30}H_{20}FNO$
M_r = 429.47
Triclinic, $P\overline{1}$
a = 9.6679 (12) Å
b = 10.1279 (12) Å
c = 12.6482 (13) Å
α = 111.420 (4)°
β = 103.871 (4)°
γ = 96.632 (5)°
V = 1090.7 (2) Å^3
Z = 2
F(000) = 448
D_x = 1.308 Mg m^{-3}
Mo $K\alpha$ radiation, λ = 0.71073 Å
Cell parameters from 5433 reflections
θ = 2.2–28.3°
μ = 0.09 mm^{-1}
T = 100 K
Block, yellow
0.17 × 0.14 × 0.10 mm

Data collection

Bruker D8 Venture diffractometer
Radiation source: INCOATEC high brilliance microfocus sealed tube
Multilayer mirror monochromator
φ and ω scans
Absorption correction: multi-scan (SADABS; Bruker, 2016)
T_{min} = 0.953, T_{max} = 0.992
47863 measured reflections
5431 independent reflections
4465 reflections with $I > 2\sigma(I)$
R_{int} = 0.057
θ_{max} = 28.3°, θ_{min} = 2.2°
h = −12→12
k = −13→13
l = −16→16

Refinement

Refinement on F^2
Least-squares matrix: full
$R[F^2 > 2\sigma(F^2)]$ = 0.044
$wR(F^2)$ = 0.111
S = 1.04
5431 reflections
298 parameters
0 restraints
Primary atom site location: dual
Hydrogen site location: inferred from neighbouring sites
H-atom parameters constrained
$w = 1/[\sigma^2(F_o^2) + (0.043P)^2 + 0.5365P]$ where $P = (F_o^2 + 2F_c^2)/3$
$(\Delta/\sigma)_{max} < 0.001$
$\Delta\rho_{max}$ = 0.35 e Å^{-3}
$\Delta\rho_{min}$ = −0.25 e Å^{-3}

Special details

Geometry. All e.s.d.'s (except the e.s.d. in the dihedral angle between two l.s. planes) are estimated using the full covariance matrix. The cell e.s.d.'s are taken into account individually in the estimation of e.s.d.'s in distances, angles and torsion angles; correlations between e.s.d.'s in cell parameters are only used when they are defined by crystal symmetry. An approximate (isotropic) treatment of cell e.s.d.'s is used for estimating e.s.d.'s involving l.s. planes.

Fractional atomic coordinates and isotropic or equivalent isotropic displacement parameters (Å^2)

	x	y	z	U_{iso}*/U_{eq}
N1	0.57874 (12)	0.61019 (11)	0.72136 (9)	0.0178 (2)
C2	0.44028 (13)	0.55330 (13)	0.65293 (11)	0.0168 (2)
C3	0.39125 (13)	0.41037 (13)	0.56278 (11)	0.0172 (2)
H3	0.2913	0.3758	0.5160	0.021*
C4	0.48798 (13)	0.32080 (13)	0.54249 (11)	0.0169 (2)
C4A	0.63845 (14)	0.37943 (14)	0.61400 (11)	0.0177 (2)
C5	0.75027 (14)	0.30146 (15)	0.60212 (12)	0.0212 (3)
H5	0.7266	0.2036	0.5449	0.025*
C6	0.89199 (15)	0.36494 (16)	0.67187 (12)	0.0248 (3)
H6	0.9654	0.3107	0.6626	0.030*
C7	0.93012 (15)	0.50959 (16)	0.75711 (12)	0.0260 (3)
H7	1.0290	0.5525	0.8047	0.031*
C8	0.82567 (14)	0.58873 (15)	0.77192 (12)	0.0230 (3)
H8	0.8523	0.6865	0.8296	0.028*
C8A	0.67734 (14)	0.52554 (13)	0.70147 (11)	0.0181 (2)
C21	0.34263 (14)	0.65308 (13)	0.67992 (11)	0.0177 (2)
H21	0.3870	0.7476	0.7408	0.021*
C22	0.19812 (14)	0.62633 (13)	0.62864 (11)	0.0186 (2)
H22	0.1478	0.5306	0.5728	0.022*
C23	0.11484 (14)	0.74090 (13)	0.65625 (11)	0.0182 (2)

O23	−0.00749 (10)	0.72442 (10)	0.59018 (8)	0.0236 (2)
C231	0.18471 (13)	0.88029 (13)	0.76569 (11)	0.0183 (2)
C232	0.22759 (15)	0.87507 (15)	0.87583 (12)	0.0240 (3)
H232	0.2164	0.7834	0.8810	0.029*
C233	0.28772 (17)	1.00315 (16)	0.98101 (12)	0.0279 (3)
H233	0.3146	0.9975	1.0563	0.034*
C234	0.30744 (15)	1.13561 (15)	0.97471 (12)	0.0249 (3)
H234	0.3483	1.2216	1.0459	0.030*
C235	0.28856 (14)	1.28262 (14)	0.85484 (13)	0.0237 (3)
H235	0.3288	1.3692	0.9256	0.028*
C236	0.25203 (15)	1.29146 (15)	0.74718 (14)	0.0262 (3)
H236	0.2674	1.3838	0.7434	0.031*
C237	0.19122 (15)	1.16382 (15)	0.64095 (13)	0.0238 (3)
H237	0.1671	1.1708	0.5661	0.029*
C238	0.16690 (13)	1.03056 (14)	0.64519 (11)	0.0194 (3)
H238	0.1245	0.9459	0.5732	0.023*
C239	0.20428 (13)	1.01680 (13)	0.75622 (11)	0.0169 (2)
C240	0.26751 (13)	1.14591 (14)	0.86303 (11)	0.0194 (3)
C41	0.44308 (14)	0.17128 (13)	0.45086 (11)	0.0192 (2)
H41	0.5086	0.1093	0.4565	0.023*
C42	0.31942 (14)	0.11400 (13)	0.36062 (11)	0.0191 (2)
H42	0.2511	0.1736	0.3563	0.023*
C421	0.28077 (13)	−0.03456 (13)	0.26718 (11)	0.0172 (2)
C422	0.13609 (14)	−0.09410 (14)	0.19403 (11)	0.0203 (3)
H422	0.0650	−0.0372	0.2051	0.024*
C423	0.09382 (14)	−0.23474 (14)	0.10539 (12)	0.0221 (3)
H423	−0.0049	−0.2750	0.0565	0.027*
C424	0.19995 (14)	−0.31374 (14)	0.09083 (11)	0.0210 (3)
F424	0.16163 (9)	−0.45148 (9)	0.00460 (7)	0.0307 (2)
C425	0.34450 (14)	−0.25893 (14)	0.15873 (12)	0.0221 (3)
H425	0.4151	−0.3159	0.1453	0.027*
C426	0.38478 (14)	−0.11893 (14)	0.24702 (11)	0.0195 (2)
H426	0.4841	−0.0795	0.2946	0.023*

Atomic displacement parameters (Å²)

	U^{11}	U^{22}	U^{33}	U^{12}	U^{13}	U^{23}
N1	0.0188 (5)	0.0167 (5)	0.0157 (5)	0.0024 (4)	0.0033 (4)	0.0058 (4)
C2	0.0192 (6)	0.0159 (6)	0.0159 (5)	0.0037 (5)	0.0054 (5)	0.0072 (5)
C3	0.0165 (6)	0.0163 (6)	0.0172 (6)	0.0020 (4)	0.0039 (4)	0.0065 (5)
C4	0.0186 (6)	0.0170 (6)	0.0158 (5)	0.0038 (5)	0.0049 (5)	0.0077 (5)
C4A	0.0188 (6)	0.0199 (6)	0.0159 (5)	0.0047 (5)	0.0051 (5)	0.0088 (5)
C5	0.0214 (6)	0.0232 (6)	0.0203 (6)	0.0076 (5)	0.0075 (5)	0.0086 (5)
C6	0.0184 (6)	0.0331 (7)	0.0255 (7)	0.0099 (5)	0.0069 (5)	0.0137 (6)
C7	0.0172 (6)	0.0333 (7)	0.0244 (7)	0.0027 (5)	0.0021 (5)	0.0120 (6)
C8	0.0203 (6)	0.0232 (6)	0.0202 (6)	0.0013 (5)	0.0020 (5)	0.0067 (5)
C8A	0.0184 (6)	0.0198 (6)	0.0157 (6)	0.0031 (5)	0.0037 (5)	0.0082 (5)
C21	0.0217 (6)	0.0136 (5)	0.0164 (6)	0.0036 (5)	0.0057 (5)	0.0048 (4)

C22	0.0212 (6)	0.0140 (5)	0.0180 (6)	0.0036 (5)	0.0049 (5)	0.0045 (5)
C23	0.0191 (6)	0.0165 (6)	0.0190 (6)	0.0034 (5)	0.0061 (5)	0.0072 (5)
O23	0.0203 (5)	0.0218 (5)	0.0247 (5)	0.0056 (4)	0.0025 (4)	0.0074 (4)
C231	0.0174 (6)	0.0189 (6)	0.0180 (6)	0.0056 (5)	0.0059 (5)	0.0058 (5)
C232	0.0292 (7)	0.0217 (6)	0.0209 (6)	0.0052 (5)	0.0071 (5)	0.0088 (5)
C233	0.0339 (8)	0.0318 (7)	0.0163 (6)	0.0075 (6)	0.0071 (5)	0.0080 (6)
C234	0.0240 (7)	0.0249 (7)	0.0182 (6)	0.0044 (5)	0.0065 (5)	0.0007 (5)
C235	0.0174 (6)	0.0177 (6)	0.0318 (7)	0.0044 (5)	0.0093 (5)	0.0042 (5)
C236	0.0226 (7)	0.0203 (6)	0.0407 (8)	0.0076 (5)	0.0131 (6)	0.0150 (6)
C237	0.0212 (6)	0.0278 (7)	0.0287 (7)	0.0095 (5)	0.0100 (5)	0.0158 (6)
C238	0.0163 (6)	0.0214 (6)	0.0208 (6)	0.0066 (5)	0.0067 (5)	0.0077 (5)
C239	0.0138 (5)	0.0174 (6)	0.0193 (6)	0.0058 (4)	0.0070 (5)	0.0054 (5)
C240	0.0149 (6)	0.0190 (6)	0.0211 (6)	0.0050 (5)	0.0066 (5)	0.0037 (5)
C41	0.0203 (6)	0.0163 (6)	0.0207 (6)	0.0063 (5)	0.0064 (5)	0.0065 (5)
C42	0.0190 (6)	0.0169 (6)	0.0207 (6)	0.0059 (5)	0.0069 (5)	0.0058 (5)
C421	0.0179 (6)	0.0163 (6)	0.0167 (6)	0.0037 (5)	0.0064 (5)	0.0053 (5)
C422	0.0169 (6)	0.0208 (6)	0.0220 (6)	0.0067 (5)	0.0064 (5)	0.0063 (5)
C423	0.0159 (6)	0.0231 (6)	0.0207 (6)	0.0026 (5)	0.0031 (5)	0.0037 (5)
C424	0.0235 (6)	0.0166 (6)	0.0175 (6)	0.0035 (5)	0.0061 (5)	0.0013 (5)
F424	0.0293 (4)	0.0210 (4)	0.0262 (4)	0.0050 (3)	0.0037 (3)	−0.0044 (3)
C425	0.0205 (6)	0.0221 (6)	0.0231 (6)	0.0095 (5)	0.0083 (5)	0.0061 (5)
C426	0.0158 (6)	0.0208 (6)	0.0198 (6)	0.0046 (5)	0.0044 (5)	0.0062 (5)

Geometric parameters (Å, º)

N1—C2	1.3323 (16)	C233—H233	0.9500
N1—C8A	1.3613 (16)	C234—C240	1.4180 (19)
C2—C3	1.4132 (17)	C234—H234	0.9500
C2—C21	1.4670 (17)	C235—C236	1.361 (2)
C3—C4	1.3799 (17)	C235—C240	1.4209 (19)
C3—H3	0.9500	C235—H235	0.9500
C4—C4A	1.4367 (17)	C236—C237	1.414 (2)
C4—C41	1.4662 (17)	C236—H236	0.9500
C4A—C5	1.4153 (17)	C237—C238	1.3658 (19)
C4A—C8A	1.4253 (17)	C237—H237	0.9500
C5—C6	1.3680 (19)	C238—C239	1.4259 (17)
C5—H5	0.9500	C238—H238	0.9500
C6—C7	1.406 (2)	C239—C240	1.4275 (17)
C6—H6	0.9500	C41—C42	1.3306 (18)
C7—C8	1.366 (2)	C41—H41	0.9500
C7—H7	0.9500	C42—C421	1.4696 (16)
C8—C8A	1.4209 (17)	C42—H42	0.9500
C8—H8	0.9500	C421—C422	1.3976 (17)
C21—C22	1.3400 (18)	C421—C426	1.4031 (17)
C21—H21	0.9500	C422—C423	1.3901 (17)
C22—C23	1.4734 (17)	C422—H422	0.9500
C22—H22	0.9500	C423—C424	1.3782 (18)
C23—O23	1.2262 (16)	C423—H423	0.9500

C23—C231	1.5065 (17)	C424—F424	1.3596 (14)
C231—C232	1.3774 (18)	C424—C425	1.3769 (18)
C231—C239	1.4258 (17)	C425—C426	1.3844 (18)
C232—C233	1.4089 (19)	C425—H425	0.9500
C232—H232	0.9500	C426—H426	0.9500
C233—C234	1.367 (2)		

C2—N1—C8A	117.60 (11)	C233—C234—C240	120.66 (12)
N1—C2—C3	123.47 (11)	C233—C234—H234	119.7
N1—C2—C21	113.66 (11)	C240—C234—H234	119.7
C3—C2—C21	122.87 (11)	C236—C235—C240	121.03 (12)
C4—C3—C2	120.25 (11)	C236—C235—H235	119.5
C4—C3—H3	119.9	C240—C235—H235	119.5
C2—C3—H3	119.9	C235—C236—C237	120.27 (13)
C3—C4—C4A	117.65 (11)	C235—C236—H236	119.9
C3—C4—C41	122.61 (11)	C237—C236—H236	119.9
C4A—C4—C41	119.74 (11)	C238—C237—C236	120.46 (13)
C5—C4A—C8A	118.15 (11)	C238—C237—H237	119.8
C5—C4A—C4	124.03 (12)	C236—C237—H237	119.8
C8A—C4A—C4	117.82 (11)	C237—C238—C239	120.91 (12)
C6—C5—C4A	120.96 (12)	C237—C238—H238	119.5
C6—C5—H5	119.5	C239—C238—H238	119.5
C4A—C5—H5	119.5	C231—C239—C238	123.28 (11)
C5—C6—C7	120.69 (13)	C231—C239—C240	118.36 (11)
C5—C6—H6	119.7	C238—C239—C240	118.34 (11)
C7—C6—H6	119.7	C234—C240—C235	121.37 (12)
C8—C7—C6	120.33 (12)	C234—C240—C239	119.67 (12)
C8—C7—H7	119.8	C235—C240—C239	118.96 (12)
C6—C7—H7	119.8	C42—C41—C4	126.28 (12)
C7—C8—C8A	120.32 (12)	C42—C41—H41	116.9
C7—C8—H8	119.8	C4—C41—H41	116.9
C8A—C8—H8	119.8	C41—C42—C421	124.84 (12)
N1—C8A—C8	117.27 (11)	C41—C42—H42	117.6
N1—C8A—C4A	123.19 (11)	C421—C42—H42	117.6
C8—C8A—C4A	119.54 (12)	C422—C421—C426	118.33 (11)
C22—C21—C2	127.55 (11)	C422—C421—C42	119.35 (11)
C22—C21—H21	116.2	C426—C421—C42	122.32 (11)
C2—C21—H21	116.2	C423—C422—C421	121.48 (12)
C21—C22—C23	122.03 (11)	C423—C422—H422	119.3
C21—C22—H22	119.0	C421—C422—H422	119.3
C23—C22—H22	119.0	C424—C423—C422	117.76 (12)
O23—C23—C22	120.72 (11)	C424—C423—H423	121.1
O23—C23—C231	120.67 (11)	C422—C423—H423	121.1
C22—C23—C231	118.59 (11)	F424—C424—C425	118.03 (11)
C232—C231—C239	120.05 (12)	F424—C424—C423	118.96 (11)
C232—C231—C23	119.30 (11)	C425—C424—C423	123.00 (12)
C239—C231—C23	120.63 (11)	C424—C425—C426	118.55 (12)
C231—C232—C233	121.24 (13)	C424—C425—H425	120.7

C231—C232—H232	119.4	C426—C425—H425	120.7
C233—C232—H232	119.4	C425—C426—C421	120.85 (12)
C234—C233—C232	119.99 (13)	C425—C426—H426	119.6
C234—C233—H233	120.0	C421—C426—H426	119.6
C232—C233—H233	120.0		

C8A—N1—C2—C3	0.80 (18)	C231—C232—C233—C234	−1.5 (2)
C8A—N1—C2—C21	−179.27 (10)	C232—C233—C234—C240	0.2 (2)
N1—C2—C3—C4	0.75 (19)	C240—C235—C236—C237	0.4 (2)
C21—C2—C3—C4	−179.17 (11)	C235—C236—C237—C238	0.8 (2)
C2—C3—C4—C4A	−1.32 (17)	C236—C237—C238—C239	−1.03 (19)
C2—C3—C4—C41	179.53 (11)	C232—C231—C239—C238	177.97 (12)
C3—C4—C4A—C5	−178.99 (12)	C23—C231—C239—C238	−3.12 (18)
C41—C4—C4A—C5	0.18 (18)	C232—C231—C239—C240	−0.56 (18)
C3—C4—C4A—C8A	0.43 (17)	C23—C231—C239—C240	178.36 (11)
C41—C4—C4A—C8A	179.61 (11)	C237—C238—C239—C231	−178.38 (12)
C8A—C4A—C5—C6	−0.59 (19)	C237—C238—C239—C240	0.15 (18)
C4—C4A—C5—C6	178.83 (12)	C233—C234—C240—C235	−179.40 (13)
C4A—C5—C6—C7	−0.1 (2)	C233—C234—C240—C239	0.85 (19)
C5—C6—C7—C8	0.3 (2)	C236—C235—C240—C234	178.98 (13)
C6—C7—C8—C8A	0.1 (2)	C236—C235—C240—C239	−1.26 (19)
C2—N1—C8A—C8	177.82 (11)	C231—C239—C240—C234	−0.66 (17)
C2—N1—C8A—C4A	−1.75 (17)	C238—C239—C240—C234	−179.26 (11)
C7—C8—C8A—N1	179.59 (12)	C231—C239—C240—C235	179.58 (11)
C7—C8—C8A—C4A	−0.83 (19)	C238—C239—C240—C235	0.98 (17)
C5—C4A—C8A—N1	−179.40 (11)	C3—C4—C41—C42	16.2 (2)
C4—C4A—C8A—N1	1.14 (18)	C4A—C4—C41—C42	−162.89 (13)
C5—C4A—C8A—C8	1.05 (18)	C4—C41—C42—C421	177.12 (12)
C4—C4A—C8A—C8	−178.41 (11)	C41—C42—C421—C422	165.01 (13)
N1—C2—C21—C22	−178.35 (12)	C41—C42—C421—C426	−16.1 (2)
C3—C2—C21—C22	1.6 (2)	C426—C421—C422—C423	1.82 (19)
C2—C21—C22—C23	−174.07 (12)	C42—C421—C422—C423	−179.21 (12)
C21—C22—C23—O23	162.87 (12)	C421—C422—C423—C424	−0.7 (2)
C21—C22—C23—C231	−15.59 (18)	C422—C423—C424—F424	−179.86 (12)
O23—C23—C231—C232	122.26 (14)	C422—C423—C424—C425	−0.8 (2)
C22—C23—C231—C232	−59.28 (16)	F424—C424—C425—C426	−179.83 (12)
O23—C23—C231—C239	−56.66 (17)	C423—C424—C425—C426	1.1 (2)
C22—C23—C231—C239	121.80 (13)	C424—C425—C426—C421	0.1 (2)
C239—C231—C232—C233	1.6 (2)	C422—C421—C426—C425	−1.50 (19)
C23—C231—C232—C233	−177.30 (12)	C42—C421—C426—C425	179.56 (12)

Hydrogen-bond geometry (Å, º)

D—H···*A*	*D*—H	H···*A*	*D*···*A*	*D*—H···*A*
C22—H22···O23^{i}	0.95	2.59	3.5407 (17)	176

C234—H234···N1^{ii}	0.95	2.67	3.5645 (18)	157
C233—H233···*Cg*2^{iii}	0.95	2.85	3.6466 (18)	142

Symmetry codes: (i) −*x*, −*y*+1, −*z*+1; (ii) −*x*+1, −*y*+2, −*z*+2; (iii) *x*, *y*+1, *z*+1.

(*E*)-3-{4-[(*E*)-2-(2-Chlorophenyl)ethenyl]quinolin-2-yl}-1-(naphthalen-1-yl)prop-2-en-1-one (IVc)

Crystal data

$C_{30}H_{20}ClNO$
M_r = 445.92
Monoclinic, $P2_1/c$
a = 3.9184 (1) Å
b = 24.6546 (8) Å
c = 21.8833 (6) Å
β = 91.271 (1)°
V = 2113.55 (10) Å^3
Z = 4
$F(000)$ = 928
D_x = 1.401 Mg m^{-3}
Mo $K\alpha$ radiation, λ = 0.71073 Å
Cell parameters from 5301 reflections
θ = 2.0–28.4°
μ = 0.21 mm^{-1}
T = 100 K
Plate, colourless
0.22 × 0.19 × 0.04 mm

Data collection

Bruker D8 Venture diffractometer
Radiation source: INCOATEC high brilliance microfocus sealed tube
Multilayer mirror monochromator
φ and ω scans
Absorption correction: multi-scan (SADABS; Bruker, 2016)
T_{min} = 0.912, T_{max} = 0.992
67339 measured reflections
5301 independent reflections
4855 reflections with $I > 2\sigma(I)$
R_{int} = 0.049
θ_{max} = 28.4°, θ_{min} = 2.0°
h = −5→5
k = −33→32
l = −29→29

Refinement

Refinement on F^2
Least-squares matrix: full
$R[F^2 > 2\sigma(F^2)]$ = 0.046
$wR(F^2)$ = 0.108
S = 1.16
5301 reflections
298 parameters
0 restraints
Primary atom site location: dual
Hydrogen site location: inferred from neighbouring sites
H-atom parameters constrained
$w = 1/[\sigma^2(F_o^2) + (0.0338P)^2 + 1.6563P]$ where $P = (F_o^2 + 2F_c^2)/3$
$(\Delta/\sigma)_{max}$ < 0.001
$\Delta\rho_{max}$ = 0.40 e Å^{-3}
$\Delta\rho_{min}$ = −0.30 e Å^{-3}

Special details

Geometry. All e.s.d.'s (except the e.s.d. in the dihedral angle between two l.s. planes) are estimated using the full covariance matrix. The cell e.s.d.'s are taken into account individually in the estimation of e.s.d.'s in distances, angles and torsion angles; correlations between e.s.d.'s in cell parameters are only used when they are defined by crystal symmetry. An approximate (isotropic) treatment of cell e.s.d.'s is used for estimating e.s.d.'s involving l.s. planes.

Fractional atomic coordinates and isotropic or equivalent isotropic displacement parameters (Å^2)

	x	*y*	*z*	U_{iso}*/U_{eq}
N1	0.3664 (3)	0.47153 (5)	0.08950 (6)	0.0161 (2)
C2	0.4073 (4)	0.46881 (6)	0.14975 (7)	0.0152 (3)
C3	0.2901 (4)	0.42458 (6)	0.18476 (6)	0.0151 (3)
H3	0.3281	0.4245	0.2278	0.018*
C4	0.1224 (4)	0.38171 (6)	0.15751 (6)	0.0143 (3)

C4A	0.0820 (4)	0.38275 (6)	0.09235 (6)	0.0145 (3)
C5	−0.0797 (4)	0.34106 (6)	0.05789 (7)	0.0176 (3)
H5	−0.1679	0.3102	0.0782	0.021*
C6	−0.1103 (4)	0.34475 (6)	−0.00471 (7)	0.0196 (3)
H6	−0.2154	0.3161	−0.0272	0.024*
C7	0.0128 (4)	0.39062 (6)	−0.03577 (7)	0.0205 (3)
H7	−0.0129	0.3929	−0.0790	0.025*
C8	0.1693 (4)	0.43198 (6)	−0.00412 (7)	0.0184 (3)
H8	0.2518	0.4627	−0.0254	0.022*
C8A	0.2082 (4)	0.42890 (6)	0.06053 (6)	0.0148 (3)
C21	0.5826 (4)	0.51511 (6)	0.17876 (7)	0.0178 (3)
H21	0.6312	0.5454	0.1535	0.021*
C22	0.6797 (4)	0.51825 (6)	0.23760 (7)	0.0174 (3)
H22	0.6425	0.4881	0.2636	0.021*
C23	0.8443 (4)	0.56778 (6)	0.26335 (7)	0.0175 (3)
O23	0.9052 (3)	0.60714 (4)	0.23118 (5)	0.0233 (2)
C231	0.9320 (4)	0.56750 (6)	0.33046 (7)	0.0168 (3)
C232	1.0670 (4)	0.52088 (6)	0.35632 (7)	0.0189 (3)
H232	1.0848	0.4891	0.3321	0.023*
C233	1.1789 (4)	0.51957 (7)	0.41798 (7)	0.0216 (3)
H233	1.2765	0.4874	0.4347	0.026*
C234	1.1465 (4)	0.56478 (7)	0.45382 (7)	0.0215 (3)
H234	1.2259	0.5639	0.4951	0.026*
C235	0.9476 (4)	0.65881 (7)	0.46783 (7)	0.0225 (3)
H235	1.0234	0.6578	0.5093	0.027*
C236	0.7928 (4)	0.70462 (7)	0.44520 (8)	0.0243 (3)
H236	0.7602	0.7351	0.4710	0.029*
C237	0.6820 (4)	0.70650 (6)	0.38349 (8)	0.0218 (3)
H237	0.5732	0.7383	0.3682	0.026*
C238	0.7287 (4)	0.66318 (6)	0.34518 (7)	0.0191 (3)
H238	0.6542	0.6654	0.3036	0.023*
C239	0.8878 (4)	0.61501 (6)	0.36721 (7)	0.0165 (3)
C240	0.9962 (4)	0.61276 (6)	0.42998 (7)	0.0185 (3)
C41	−0.0132 (4)	0.33695 (6)	0.19433 (7)	0.0161 (3)
H41	−0.0355	0.3021	0.1762	0.019*
C42	−0.1064 (4)	0.34340 (6)	0.25235 (7)	0.0162 (3)
H42	−0.0755	0.3785	0.2695	0.019*
C421	−0.2508 (4)	0.30209 (6)	0.29209 (6)	0.0152 (3)
C422	−0.4071 (4)	0.31632 (6)	0.34698 (7)	0.0178 (3)
Cl42	−0.43548 (11)	0.38464 (2)	0.36900 (2)	0.02615 (11)
C423	−0.5499 (4)	0.27812 (7)	0.38518 (7)	0.0225 (3)
H423	−0.6526	0.2891	0.4221	0.027*
C424	−0.5418 (4)	0.22379 (7)	0.36909 (7)	0.0237 (3)
H424	−0.6434	0.1974	0.3946	0.028*
C425	−0.3846 (4)	0.20784 (7)	0.31554 (7)	0.0216 (3)
H425	−0.3754	0.1705	0.3048	0.026*
C426	−0.2418 (4)	0.24645 (6)	0.27795 (7)	0.0179 (3)
H426	−0.1348	0.2351	0.2416	0.021*

Atomic displacement parameters (Å²)

	U^{11}	U^{22}	U^{33}	U^{12}	U^{13}	U^{23}
N1	0.0176 (6)	0.0149 (6)	0.0158 (6)	0.0018 (5)	0.0016 (5)	0.0015 (5)
C2	0.0146 (6)	0.0152 (7)	0.0159 (7)	0.0019 (5)	0.0004 (5)	−0.0005 (5)
C3	0.0159 (6)	0.0166 (7)	0.0128 (6)	0.0018 (5)	0.0005 (5)	0.0008 (5)
C4	0.0132 (6)	0.0156 (6)	0.0142 (6)	0.0028 (5)	0.0011 (5)	0.0009 (5)
C4A	0.0137 (6)	0.0153 (6)	0.0145 (6)	0.0032 (5)	0.0015 (5)	0.0000 (5)
C5	0.0181 (7)	0.0174 (7)	0.0174 (7)	0.0003 (5)	0.0004 (5)	0.0006 (5)
C6	0.0214 (7)	0.0205 (7)	0.0169 (7)	0.0004 (6)	−0.0028 (6)	−0.0031 (6)
C7	0.0246 (7)	0.0230 (8)	0.0140 (7)	0.0048 (6)	0.0008 (6)	−0.0001 (6)
C8	0.0212 (7)	0.0192 (7)	0.0148 (7)	0.0044 (6)	0.0021 (5)	0.0032 (5)
C8A	0.0154 (6)	0.0151 (6)	0.0139 (6)	0.0038 (5)	0.0014 (5)	0.0004 (5)
C21	0.0194 (7)	0.0149 (7)	0.0193 (7)	0.0001 (5)	0.0038 (5)	0.0005 (5)
C22	0.0191 (7)	0.0148 (7)	0.0185 (7)	−0.0017 (5)	0.0032 (5)	−0.0002 (5)
C23	0.0180 (7)	0.0165 (7)	0.0180 (7)	0.0004 (5)	0.0025 (5)	−0.0009 (5)
O23	0.0323 (6)	0.0167 (5)	0.0209 (6)	−0.0036 (4)	0.0021 (5)	0.0012 (4)
C231	0.0153 (6)	0.0171 (7)	0.0180 (7)	−0.0021 (5)	0.0015 (5)	0.0002 (5)
C232	0.0202 (7)	0.0165 (7)	0.0201 (7)	0.0003 (5)	0.0025 (6)	−0.0005 (6)
C233	0.0210 (7)	0.0208 (7)	0.0231 (8)	0.0017 (6)	−0.0003 (6)	0.0057 (6)
C234	0.0213 (7)	0.0266 (8)	0.0166 (7)	−0.0010 (6)	−0.0018 (6)	0.0033 (6)
C235	0.0261 (8)	0.0250 (8)	0.0164 (7)	−0.0043 (6)	0.0030 (6)	−0.0031 (6)
C236	0.0296 (8)	0.0198 (7)	0.0238 (8)	−0.0040 (6)	0.0084 (6)	−0.0052 (6)
C237	0.0246 (8)	0.0166 (7)	0.0246 (8)	0.0001 (6)	0.0055 (6)	0.0008 (6)
C238	0.0208 (7)	0.0182 (7)	0.0183 (7)	−0.0011 (6)	0.0032 (6)	0.0007 (6)
C239	0.0153 (6)	0.0164 (7)	0.0178 (7)	−0.0030 (5)	0.0024 (5)	0.0007 (5)
C240	0.0181 (7)	0.0191 (7)	0.0185 (7)	−0.0043 (5)	0.0026 (5)	−0.0008 (6)
C41	0.0175 (7)	0.0158 (7)	0.0150 (7)	−0.0001 (5)	−0.0011 (5)	0.0010 (5)
C42	0.0172 (6)	0.0156 (7)	0.0158 (7)	0.0008 (5)	0.0002 (5)	0.0003 (5)
C421	0.0136 (6)	0.0199 (7)	0.0122 (6)	0.0016 (5)	−0.0018 (5)	0.0026 (5)
C422	0.0173 (7)	0.0208 (7)	0.0152 (7)	0.0031 (5)	−0.0012 (5)	0.0004 (5)
Cl42	0.0349 (2)	0.0250 (2)	0.01872 (18)	0.00561 (16)	0.00466 (15)	−0.00432 (14)
C423	0.0197 (7)	0.0333 (9)	0.0146 (7)	0.0022 (6)	0.0019 (6)	0.0041 (6)
C424	0.0189 (7)	0.0311 (9)	0.0211 (8)	−0.0033 (6)	−0.0029 (6)	0.0121 (6)
C425	0.0216 (7)	0.0204 (7)	0.0224 (8)	−0.0017 (6)	−0.0053 (6)	0.0041 (6)
C426	0.0180 (7)	0.0196 (7)	0.0160 (7)	0.0010 (5)	−0.0005 (5)	0.0009 (5)

Geometric parameters (Å, º)

N1—C2	1.3263 (19)	C233—H233	0.9500
N1—C8A	1.3687 (19)	C234—C240	1.416 (2)
C2—C3	1.415 (2)	C234—H234	0.9500
C2—C21	1.469 (2)	C235—C236	1.369 (2)
C3—C4	1.374 (2)	C235—C240	1.421 (2)
C3—H3	0.9500	C235—H235	0.9500
C4—C4A	1.4314 (19)	C236—C237	1.410 (2)
C4—C41	1.4726 (19)	C236—H236	0.9500
C4A—C5	1.416 (2)	C237—C238	1.373 (2)

C4A—C8A	1.428 (2)	C237—H237	0.9500
C5—C6	1.375 (2)	C238—C239	1.421 (2)
C5—H5	0.9500	C238—H238	0.9500
C6—C7	1.410 (2)	C239—C240	1.430 (2)
C6—H6	0.9500	C41—C42	1.338 (2)
C7—C8	1.370 (2)	C41—H41	0.9500
C7—H7	0.9500	C42—C421	1.461 (2)
C8—C8A	1.422 (2)	C42—H42	0.9500
C8—H8	0.9500	C421—C422	1.405 (2)
C21—C22	1.337 (2)	C421—C426	1.407 (2)
C21—H21	0.9500	C422—C423	1.385 (2)
C22—C23	1.486 (2)	C422—Cl42	1.7563 (16)
C22—H22	0.9500	C423—C424	1.386 (2)
C23—O23	1.2254 (18)	C423—H423	0.9500
C23—C231	1.501 (2)	C424—C425	1.393 (2)
C231—C232	1.381 (2)	C424—H424	0.9500
C231—C239	1.434 (2)	C425—C426	1.384 (2)
C232—C233	1.410 (2)	C425—H425	0.9500
C232—H232	0.9500	C426—H426	0.9500
C233—C234	1.370 (2)		

C2—N1—C8A	117.72 (12)	C233—C234—C240	120.78 (14)
N1—C2—C3	122.93 (13)	C233—C234—H234	119.6
N1—C2—C21	115.80 (13)	C240—C234—H234	119.6
C3—C2—C21	121.27 (13)	C236—C235—C240	120.82 (15)
C4—C3—C2	121.04 (13)	C236—C235—H235	119.6
C4—C3—H3	119.5	C240—C235—H235	119.6
C2—C3—H3	119.5	C235—C236—C237	119.87 (15)
C3—C4—C4A	117.39 (13)	C235—C236—H236	120.1
C3—C4—C41	120.93 (13)	C237—C236—H236	120.1
C4A—C4—C41	121.68 (13)	C238—C237—C236	121.12 (15)
C5—C4A—C8A	118.32 (13)	C238—C237—H237	119.4
C5—C4A—C4	123.77 (13)	C236—C237—H237	119.4
C8A—C4A—C4	117.91 (13)	C237—C238—C239	120.44 (15)
C6—C5—C4A	120.69 (14)	C237—C238—H238	119.8
C6—C5—H5	119.7	C239—C238—H238	119.8
C4A—C5—H5	119.7	C238—C239—C240	118.51 (14)
C5—C6—C7	120.66 (14)	C238—C239—C231	123.38 (14)
C5—C6—H6	119.7	C240—C239—C231	118.05 (13)
C7—C6—H6	119.7	C234—C240—C235	120.87 (14)
C8—C7—C6	120.48 (14)	C234—C240—C239	119.91 (14)
C8—C7—H7	119.8	C235—C240—C239	119.22 (14)
C6—C7—H7	119.8	C42—C41—C4	122.64 (14)
C7—C8—C8A	120.02 (14)	C42—C41—H41	118.7
C7—C8—H8	120.0	C4—C41—H41	118.7
C8A—C8—H8	120.0	C41—C42—C421	126.81 (14)
N1—C8A—C8	117.21 (13)	C41—C42—H42	116.6
N1—C8A—C4A	122.97 (13)	C421—C42—H42	116.6

C8—C8A—C4A	119.82 (13)	C422—C421—C426	116.41 (13)
C22—C21—C2	125.56 (14)	C422—C421—C42	121.12 (14)
C22—C21—H21	117.2	C426—C421—C42	122.46 (13)
C2—C21—H21	117.2	C423—C422—C421	122.40 (15)
C21—C22—C23	121.64 (14)	C423—C422—Cl42	117.23 (12)
C21—C22—H22	119.2	C421—C422—Cl42	120.36 (12)
C23—C22—H22	119.2	C422—C423—C424	119.46 (15)
O23—C23—C22	121.42 (14)	C422—C423—H423	120.3
O23—C23—C231	121.50 (14)	C424—C423—H423	120.3
C22—C23—C231	117.08 (13)	C423—C424—C425	120.01 (15)
C232—C231—C239	120.00 (14)	C423—C424—H424	120.0
C232—C231—C23	118.82 (13)	C425—C424—H424	120.0
C239—C231—C23	121.16 (13)	C426—C425—C424	119.86 (15)
C231—C232—C233	121.29 (14)	C426—C425—H425	120.1
C231—C232—H232	119.4	C424—C425—H425	120.1
C233—C232—H232	119.4	C425—C426—C421	121.84 (14)
C234—C233—C232	119.89 (14)	C425—C426—H426	119.1
C234—C233—H233	120.1	C421—C426—H426	119.1
C232—C233—H233	120.1		

C8A—N1—C2—C3	−1.1 (2)	C232—C233—C234—C240	1.1 (2)
C8A—N1—C2—C21	179.16 (12)	C240—C235—C236—C237	−0.5 (2)
N1—C2—C3—C4	−0.6 (2)	C235—C236—C237—C238	−0.5 (2)
C21—C2—C3—C4	179.15 (13)	C236—C237—C238—C239	0.6 (2)
C2—C3—C4—C4A	2.1 (2)	C237—C238—C239—C240	0.2 (2)
C2—C3—C4—C41	−177.15 (13)	C237—C238—C239—C231	177.35 (14)
C3—C4—C4A—C5	178.86 (13)	C232—C231—C239—C238	−175.36 (14)
C41—C4—C4A—C5	−1.9 (2)	C23—C231—C239—C238	6.6 (2)
C3—C4—C4A—C8A	−2.02 (19)	C232—C231—C239—C240	1.8 (2)
C41—C4—C4A—C8A	177.26 (13)	C23—C231—C239—C240	−176.23 (13)
C8A—C4A—C5—C6	0.8 (2)	C233—C234—C240—C235	176.98 (15)
C4—C4A—C5—C6	179.89 (14)	C233—C234—C240—C239	−2.3 (2)
C4A—C5—C6—C7	−1.2 (2)	C236—C235—C240—C234	−178.02 (15)
C5—C6—C7—C8	0.9 (2)	C236—C235—C240—C239	1.3 (2)
C6—C7—C8—C8A	−0.1 (2)	C238—C239—C240—C234	178.16 (14)
C2—N1—C8A—C8	−179.29 (13)	C231—C239—C240—C234	0.9 (2)
C2—N1—C8A—C4A	1.1 (2)	C238—C239—C240—C235	−1.2 (2)
C7—C8—C8A—N1	−179.95 (14)	C231—C239—C240—C235	−178.45 (14)
C7—C8—C8A—C4A	−0.4 (2)	C3—C4—C41—C42	27.2 (2)
C5—C4A—C8A—N1	179.58 (13)	C4A—C4—C41—C42	−152.07 (14)
C4—C4A—C8A—N1	0.4 (2)	C4—C41—C42—C421	178.41 (13)
C5—C4A—C8A—C8	0.0 (2)	C41—C42—C421—C422	−165.79 (15)
C4—C4A—C8A—C8	−179.14 (13)	C41—C42—C421—C426	14.2 (2)
N1—C2—C21—C22	−173.04 (14)	C426—C421—C422—C423	−0.8 (2)
C3—C2—C21—C22	7.2 (2)	C42—C421—C422—C423	179.18 (14)
C2—C21—C22—C23	−177.62 (14)	C426—C421—C422—Cl42	−179.56 (11)
C21—C22—C23—O23	−1.9 (2)	C42—C421—C422—Cl42	0.5 (2)
C21—C22—C23—C231	177.99 (14)	C421—C422—C423—C424	−0.4 (2)

O23—C23—C231—C232	−139.12 (16)	Cl42—C422—C423—C424	178.40 (12)
C22—C23—C231—C232	41.01 (19)	C422—C423—C424—C425	1.4 (2)
O23—C23—C231—C239	38.9 (2)	C423—C424—C425—C426	−1.1 (2)
C22—C23—C231—C239	−140.95 (14)	C424—C425—C426—C421	−0.2 (2)
C239—C231—C232—C233	−3.1 (2)	C422—C421—C426—C425	1.1 (2)
C23—C231—C232—C233	174.98 (14)	C42—C421—C426—C425	−178.92 (14)
C231—C232—C233—C234	1.6 (2)		

Hydrogen-bond geometry (Å, º)

D—H···*A*	*D*—H	H···*A*	*D*···*A*	*D*—H···*A*
C8—H8···N1^{i}	0.95	2.63	3.551 (2)	163
C425—H425···O23^{ii}	0.95	2.55	3.290 (2)	134

Symmetry codes: (i) −*x*+1, −*y*+1, −*z*; (ii) −*x*+1, *y*−1/2, −*z*+1/2.